Assessment of the use of brightfield microscopy for producing normative ranges for intraepidermal nerve fibre density in the dog

Thesis submitted in fulfilment of the requirements of the University of Glasgow for the degree of Master of Veterinary Medicine

by

Gail Elaine Chapman

BVM&S, PhD, MRCVS

School of Veterinary Medicine,

College of Medical, Veterinary and Life Sciences

August 2020

Abstract

Intra-epidermal nerve fibre (IENF) quantification is a useful tool which aids the diagnosis of small fibre neuropathies in human patients. This study aimed to investigate the practicality of IENF quantification in dogs, using skin biopsies from the distal limb. Technical methods for staining of nerve fibres were optimised and two IENF quantification protocols investigated. The utility of formalin fixation versus a standard fixative used in human medicine (Zamboni's fixative) was assessed and an attempt was made to determine baseline values for IENF density (IENFD) in dogs without peripheral nerve disease.

Reproducibility of IENFD was poor: whilst intra-observer reproducibility for the same set of sections was reasonable, intra-sample reproducibility on a second set of sections did not show correlation with the first. Additionally, the overall density of fibres in canine haired skin was low, meaning that a very high level of reproducibility would be required to recommend a suitable diagnostic cut-off value. Increasing the length of epidermis quantified to ≥40 mm did not significantly improve intra-sample reproducibility.

Therefore, using the methods described here it is unlikely that the quantification of IENF in the haired skin of the dog can be used as a diagnostic test in peripheral nerve disease. Investigation of IENF quantification using immunofluorescence techniques and/or assessing the canine footpad, as an alternative to haired skin, may be warranted.

Table of Contents

List of Tables

List of Figures

Acknowledgements

I would like to thank my supervisor, Angie Rupp, without whom this thesis would not have been possible, for her vision and guidance throughout, and ongoing. Thanks go also to Alexander Gray, Caroline Millins, Francesco Marchesi and Pamela Johnston for their support and advice.

Special thanks go to the dog owners, veterinarians and post mortem room staff involved in donation and obtaining of samples used in this study, in particular, Michael McGuigan, Alexander Gray, Jo Morris, Patrick Smith and Mariana Lopes.

Thanks go to the histopathology staff Frazer Bell, Lynn Oxford, Niamh Armstrong and especially Lynn Stevenson, for their technical help, patience and moral support. Thanks also to Lynne Fleming for preparation of Zamboni's solution and to Lynne, Ana Monteiro and Jennifer Barrie for their support and advice in the laboratory.

Special thanks go to Mark McLaughlin for allowing me to use his laboratory equipment and space, and to Lauren Black for sharing it with such charm. Likewise, Ronnie Barron for allowing me to invade his office, and himself and Jakob for providing images for the sampling instructions.

Thanks go to the University of Glasgow for their generous financial support during my residency and to the Veterinary Small Grants Fund for funding the work in this thesis.

Thanks also, to my fellow residents for their moral support and friendship.

To my wonderful husband, Mark, for his support, patience and love. Again.

"Think like a (wo)man of action. Act like a (wo)man of thought." – Henry Bergson

I declare that, except where explicit reference is made to the contribution of others, that this dissertation is the result of my own work and has not been submitted for any other degree at the University of Glasgow or any other institution.

Gail Chapman

List of Abbreviations

ACP	acute canine polyradiculoneuritis
BM	basement membrane
°C	degrees Celsius (Centigrade)
CIDP	chronic inflammatory demyelinating polyneuropathy
CV	coefficient of variation (typical percentage error)
EFNS	European Federation of Neurological Sciences
FB	formalin fixed sample from the proximal site
FE	entire female
FN	neutered female
FT	formalin fixed sample from the distal site
g	grams
GBS	Guillain-Barré syndrome
GSD	German shepherd dog
IENF	intraepidermal nerve fibre(s)
IENFD	intraepidermal nerve fibre density
IHC	immunohistochemistry
IR	interquartile range
l	litres
LoA	limit(s) of agreement
MD	minimum difference to be considered ‘real’
ME	entire male
MN	neutered male

ml	millilitres
mm	millimetres
NBF	neutral buffered formalin
NHS	normal horse serum
PBS	phosphate buffered saline
PLP	paraformaldehyde-lysine periodate
PME	post mortem examination
PMI	post mortem interval
PVP	polyvinylpyrrolidone
RC	repeatability coefficient
RIV	relative inter-trial variability
rpm	revolutions per minute
SEM	standard error of the measure
TE	typical error
TBST	0.1% Tween-20 in tris buffered saline
ZT	Zamboni's fixed sample from the proximal site
ZB	Zamboni's fixed sample from the distal site
µm	micrometres

1. INTRODUCTION

Skin biopsy and more specifically quantification of intra-epidermal nerve fibres (IENF) in the skin has been used to support a diagnosis of small fibre sensory neuropathies in people since at least 1989 (Levy et al., 1989), but has not yet been utilised as a diagnostic tool in veterinary medicine. In people, such examinations are recommended when clinical and neurophysiological examination do not allow for definitive diagnosis, but the patient has burning pain in the lower limbs (Herrmann et al., 1999; Sommer, 2017). Length (of nerve) dependent (commonly degenerative conditions) versus non-length dependent conditions (such as inflammatory or immune-mediated conditions) can be differentiated if proximal and distal samples are taken (Üçeyler et al., 2010).

Innervation of the Skin

Neurons of dorsal root ganglia, parasympathetic and sympathetic ganglia send nerve fibres to the skin, where they terminate at sweat glands, hair follicles and blood vessels, supply Meissner's corpuscles and Merkel cells, and innervate the epidermis (Sommer, 2019) (motor fibres innervating the arrector pili muscles are not here discussed). These fibres are classified Aβ, Aδ or C-fibres based on diameter and conduction velocity; Aβ-fibres representing large fibres with high conduction velocity, C-fibres having small diameter and low conduction velocity and Aδ-fibres being intermediate in diameter and conduction velocity. The term 'small fibres' includes both C-fibres and Aδ-fibres. A-fibres are myelinated and C-fibres are unmyelinated (McGlone and Reilly, 2010). Ninety per cent of sensory axons in the skin are unmyelinated C-fibres which include pain, tactile and autonomic fibres; the remaining 10% of myelinated sensory fibres, include Aδ-fibres (pain, thermal) and Aβ-fibres (low-threshold mechanoreceptors) (McGlone and Reilly, 2010; Sommer, 2019).

Nerve fibre bundles, in their majority comprising unmyelinated sensory fibres, extend towards superficial through the dermis, form sub-epidermal plexuses, then penetrate the epidermal basement membrane, losing their Schwann cell covering and coursing between keratinocytes ("free nerve endings"). These sensory C-fibres, and fewer Aδ sensory fibres, are termed intra-epidermal nerve fibres (Mangus et al., 2019). The pattern of epidermal innervation in dogs is described as broadly similar to that of humans (Alves de Medeiros et al., 2009).

PERIPHERAL NERVE DISEASE AND IENF QUANTIFICATION IN HUMANS

IENF quantification in humans can be used to assess neuropathies in various conditions or groups of conditions, for example metabolic disease (diabetic neuropathy and hypothyroidism), degenerative disease (such as idiopathic small fibre sensory neuropathy, sensory ganglionopathies, Parkinson's disease and inherited conditions), immune-mediated disease (such as inflammatory demyelinating neuropathies and neuropathies associated with systemic auto-immune diseases), infectious disease (e.g. HIV, leprosy), or toxin exposure (e.g. chemotherapeutic agents), and are used to examine nerve fibre regeneration after chemical or traumatic injury (Mellgren et al., 2013). In general, intra-epidermal nerve fibre density (IENFD) is reduced in these peripheral nerve diseases and therefore normative ranges have been used to produce a 'normality cut-off' which represents a minimum IENFD to be considered normal, often using the 5th percentile (Bakkers et al., 2009; Collongues et al., 2018; McArthur et al., 1998; Provitera et al., 2016). Frequently however, increased branching within the epidermis is seen in neuropathy patients, and therefore international guidelines for IENF quantification recommend that nerves that branch after crossing the epidermal basement membrane are counted as one (Kennedy et al., 2005; Lauria et al., 2005a).

In diabetes mellitus, reduced intra-epidermal nerve fibre density is used to identify early neuropathy and monitor progression (Løseth et al., 2008; Mellgren et al., 2013). Hypothyroidism is also associated with IENF depletion in some cases (Nebuchennykh et al., 2010). Idiopathic small fibre sensory neuropathy is associated with burning sensation in the feet, sometimes reduced pain sensation and progressive reduction in IENFD at the calf (Lauria et al., 2003) and in these cases IENF quantification is more sensitive than nerve biopsy or quantitative sensory testing (Herrmann et al., 1999; Mellgren et al., 2013). Sensory ganglionopathies cause widespread proprioceptive deficits, ataxia and IENF loss without a proximodistal gradient, helping distinguish ganglionopathies from axonal neuropathies (Lauria et al., 2001). In immune-mediated myelinopathies, such as the demyelinating forms of GBS and CIDP, axonal density and thus IENFD is reduced in many patients and depletion is associated with poorer outcomes (Chiang et al., 2002; Ruts et al., 2012). In GBS specifically, epidermal fibre depletion occurs early in the disease and has been correlated with pain (Lauria et al., 2010b). In other neuropathies associated with autoimmune diseases, such as systemic

lupus erythematosus and Sjogren's syndrome, reduction in IENFD is also seen (Chai et al., 2005; Tseng et al., 2006), as well as in several inherited neuropathies predominantly involving small fibres such as Fabry's disease (Torvin Møller et al., 2009), familial dysautonomia (Hilz et al., 2004), and congenital insensitivity of pain (Nolano et al., 2000). Furthermore IENF quantification is also used in the diagnostic work-up of HIV patients; neuropathy may be HIV-associated or caused by neurotoxic antiretroviral drugs (Herrmann et al., 1999; Mellgren et al., 2013). Finally, IENFD may be reduced in leprosy (Facer et al., 1998) and Parkinson's disease (Mellgren et al., 2013). Interestingly, patients with spinal onset amyotrophic lateral sclerosis (ALS, motor neuron disease) often have reduced IENFD at the distal leg, whilst those with bulbar onset do not initially (Truini et al., 2015; Weis et al., 2011).

International guidelines have been published for the use of skin biopsies to support a diagnosis of small fibre neuropathies in humans. These focus on the acquisition of the biopsy, fixation methods, tissue processing and immunohistochemistry for IENF quantification (Lauria et al., 2010a). Also specific counting rules for IENF have been described (Lauria et al., 2005a; Mangus et al., 2019). Protein gene product 9.5 (PGP9.5), also known as ubiquitin carboxyl-terminal esterase L1, is an enzyme expressed in the cytoplasm of neurons and is the most common antigenic target used to immunostain axons in IENF assessments.

Peripheral Nerve Disease in Dogs

Several peripheral nerve diseases occur in dogs, for which IENF quantification may facilitate diagnosis or progression monitoring. The prevalence of canine diabetic neuropathy is unknown and subclinical disease is believed most common (Mariani, 2017). Demyelination causing axonal degeneration is characteristic in humans and dogs (Fracassi, 2017; Morgan et al., 2008) so IENFD depletion may be expected in dogs, as for humans. In hypothyroidism, neuromuscular dysfunction is described and nerve biopsies may show demyelination and axonal degeneration in specific nerves. Also, cranial nerves are often affected and in some cases, limb paresis is seen (Mariani, 2017) which may correspond to IENF depletion, as described in humans. Sensory polyganglioradiculoneuritis of unknown cause (Chrisman et al., 1999; Cummings et al., 1983; Funamoto et al., 2007) causes axonal degeneration of dorsal root ganglia and sensory nerves, therefore IENF is likely to be reduced. Acute canine

polyradiculoneuritis (ACP) is considered to represent an immune-mediated disease with similarity to GBS. Hyperaesthesia (indicating a specifically sensory component of this disease) is reported in dogs (Cuddon, 2002; Cummings and Haas, 1966; Rupp et al., 2013), making it likely that IENFD is reduced in some ACP cases, similar to GBS-patients. Canine CIDP is characterised by demyelination and axonal degeneration is seen less frequently (Mariani, 2017). However, IENF depletion affects some human patients, hence possibly also dogs. Additionally, several idiopathic or hereditary, mixed or sensory peripheral polyneuropathies such as distal denervating disease (Griffiths and Duncan, 1979) and progressive axonopathy of Boxers (Griffiths et al., 1986) are also described in dogs, for which it is unclear if, or to what extent IENF would be affected. Toxic neuropathies may also reduce IENFD; for example, the common veterinary chemotherapy agent vincristine causes degeneration in unmyelinated fibres (Braund, 2003). Paraneoplastic neuropathy representing an immune-mediated response to antigen mimicry of the neoplasm is described in the dog, however predominantly presents with motor signs (Mariani, 2017). Should autoantibodies in this specific disease entity be directed against myelin or other antigens present in sensory nerves, then reduction in IENFD may be possible. Furthermore, protozoal polyradiculoneuritis which is typically considered a neuromuscular disorder causing interstitial inflammation of peripheral nerves and muscles may potentially, if substantial enough, result in reduced IENFD, although to the author's knowledge this has not been studied.

Current Diagnosis of Peripheral Nerve Disease in Dogs

In animals, clear clinical signs of sensory neuropathy are restricted to apparent changes in pain perception and proprioceptive deficits (in contrast to people where touch and temperature perception can be described by the patient), and neuropathies with a sensory component may be associated with self-mutilation (Braund, 2003). When peripheral neuropathy is suspected based on clinical history and neurological examination, haematology, biochemistry and urinalysis can be used to investigate possible underlying systemic disease such as diabetes mellitus or hypothyroidism and may in rare cases indicate an immune-mediated basis for suspected neuropathy. Directed blood tests for these conditions can then be applied, such as blood glucose levels, hormone levels and serology. Imaging of the thorax and abdomen may be used to investigate the possibility of paraneoplastic neuropathy. Cerebrospinal fluid

analysis may be useful in the supporting the presence of some infectious and autoimmune-mediated very proximal peripheral neuropathies (Cuddon, 2002). If a diagnosis has not been reached, then electrophysiological assessment of peripheral nerves and nerve roots, and muscle and nerve biopsy can be considered. Tests used to specifically evaluate the sensory nervous system include direct sensory nerve stimulation and cord dorsum potential (described in Lorenz et al., 2011) however, access to and expertise in the use of electrodiagnostic equipment is uncommon in first opinion practice (Alves de Medeiros et al., 2009). The final refinement of the differential diagnoses may be made based on the results of electrophysiological assessments in conjunction with histopathology of nerve biopsy and possibly muscle biopsy (Cuddon, 2002).

ADVANTAGES OF IENF QUANTIFICATION

Skin biopsy is considered safe, simple and can be repeated to assess disease progression. For this reason, it has gained popularity in human medicine in recent years. By comparison, in a study of sural and peroneal nerve biopsy, significant numbers of complications were seen, including post-operative pain (30%), paraesthesia (40%) and dysaesthesia (33%), which lasted longer than 18 months in some cases (Gabriel, 2000; Hilton et al., 2007). Consequently, it is recommended that nerve biopsy be avoided unless neuropathy is a significant problem to the patient and there is a specific question which cannot be answered otherwise (Hughes, 2014; Said, 2002). In people, the main indication for taking a nerve biopsy is interstitial pathology of the nerve trunk, inflammation of infectious or immune-mediated origin, vasculitis and ensuing issues with blood flow (Davies et al., 1996), amyloidosis (Said, 2002), or intrafascicular neoplastic disease. Many human cases of neuropathy, however, can be diagnosed without nerve biopsy (Sommer, 2017). In both people and dogs, nerve biopsy generally requires general anaesthesia, whilst skin biopsy can be achieved under sedation and local anaesthesia in most dogs, reducing cost and minimising anaesthetic risk.

To the author’s knowledge only two previous studies describing immunohistological examination of canine skin biopsies for the presence of intraepidermal nerve fibres and their quantification have been published. One study used formalin fixed, paraffin embedded tissues and immunofluorescence staining for beta-3 tubulin, and IENFs

were only rarely visualised in normal haired canine skin (Laprais et al., 2017). The other study applied methods similar to those recommended and used in human studies (Zamboni's fixed tissues examined by brightfield microscopy and nerves stained with PGP 9.5), however, examined thinner sections than recommended, overall investigating IENFs in the haired skin of ten healthy 15 month old beagles, thus reporting normative data on a very limited canine population only (Alves de Medeiros et al., 2009).

Aims of this Thesis

Skin biopsy is a simple and common procedure used in assessment of small fibre (commonly sensory) neuropathies in humans and, therefore, represents a potentially useful option for further investigation of suspected small fibre neuropathies in the dog.

This purpose of this study was to examine the practicality and feasibility of IENF quantification and to accumulate normative data for dogs of various breeds and ages, using skin biopsies from the distal hind limbs of animals which were not suspected to have peripheral nerve disease. Whilst two previous studies were conducted in dogs for investigation of IENF (see above), only one of these produced fibre densities and this study was limited to examining ten dogs of the same age and breed (Alves de Medeiros et al., 2009; Laprais et al., 2017).

The main objectives were to optimise technical methods for IENF quantification, investigate the practicality of different fixation methods and to determine baseline values for IENFD in dogs without peripheral nerve disease. Aspects to be optimised included tissue fixation, sectioning, permeabilization and immunohistochemical staining. In particular, the potential for use of formalin fixation was to be investigated, formalin being more easily available to veterinarians when compared to the fixatives recommended in human protocols. Protocols for measuring epidermal length and counting intra-epidermal nerve fibres were also to be assessed for practicality and feasibility in the canine skin. Additionally, this study hoped to examine the effect of subject characteristics such as age and sex on IENFD.

2. MATERIALS AND METHODS

Sampling

Ethical approval for this study was obtained from the University of Glasgow School of Veterinary Medicine Ethics Committee (reference 13a/17).

Cadaver skin samples were obtained by the researcher *and local veterinarians.* Samples obtained by the researcher comprised skin samples from dogs submitted to Veterinary Diagnostic Services, School of Veterinary Medicine, University of Glasgow for post mortem examination (animals cleared for research purposes) within 24 hours of death without (known or suspected) peripheral nerve disease. Skin samples obtained by contributing veterinarians were collected immediately after euthanasia from dogs without suspected peripheral nerve disease and with owner consent (see Appendix A).

From each cadaver 4 skin samples were obtained using a 3 or 6 mm biopsy punch. These comprised two adjacent samples from the area just caudal to the lateral aspect of the stifle joint, i.e. the site corresponding to skin overlying the common peroneal nerve biopsy site, and two adjacent samples from the distal lateral aspect of the tibia at 1/3 of the way up the lower leg from the lateral malleolus (Figure 2.1). Sampling instructions for submitting veterinarians are included in Appendix A.

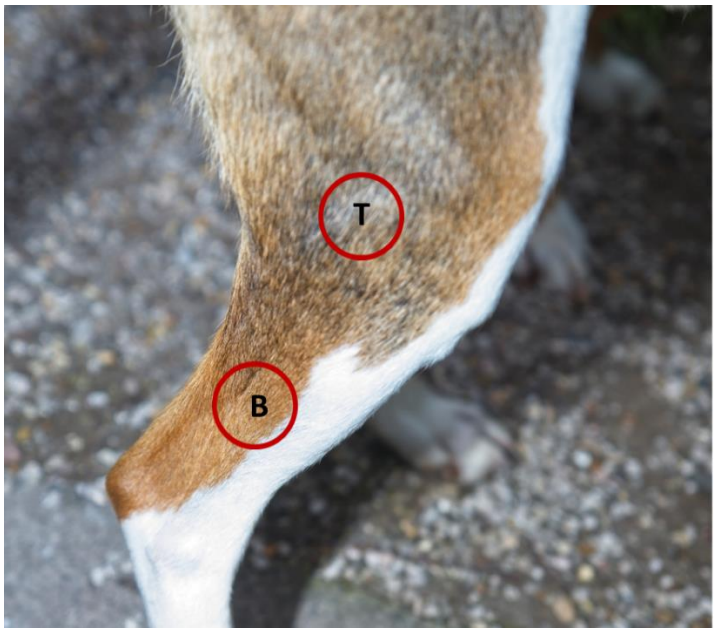

Figure 2.1 Skin sample sites.
T – proximal site; caudal to the lateral aspect of the stifle joint. B – distal site; at the distal third of the lateral aspect of the tibia.

Samples were placed with the subcutical aspect downwards on cardboard and immediately submerged in fixative in prefilled and prelabelled sample pots, resulting in subject (dog) numbers not being consecutive. Pots were additionally labelled ZT (Zamboni's - proximal site), ZB (Zamboni's - distal site), FT (10 % neutral buffered formalin (NBF) - proximal site) and FB (NBF – distal site).

For each dog, the following information was recorded: date of sampling, signalment and sampling interval (post mortem interval - PMI). Additionally, a summary of the medical history from the post mortem examination (PME) submission form and body condition score was recorded for samples from dogs undergoing PME whilst a short questionnaire on medical history was included in the consent form for submitted samples (Figure 2.2).

Does the animal have diabetes mellitus? Y/N:
Does the animal have a peripheral neuropathy? Y/N:
If yes, then what neuropathy has been diagnosed (if known)?
Has the animal recently received chemotherapy? Y/N
Is the animal hypothyroid? Y/N

Figure 2.2 Medical history questionnaire.

Fixation

2.2.1 Choice of Fixatives

The most commonly used fixatives for IENFD measurement in skin biopsies are 2% paraformaldehyde-lysine periodate (PLP) and Zamboni's fixative (2% paraformaldehyde and picric acid) (Mellgren et al., 2013). Although 2% PLP reportedly represents the fixative most often used for brightfield microscopy, it has the disadvantage that it must be kept refrigerated and is best made up fresh before use, so was not considered practical for this study. Zamboni's fixative on the other hand, which is stable and can be stored at room temperature (Hays et al., 2016), was considered suitable for supplying to submitting veterinarians. Since the study objective was to investigate whether IENFD could be used as a test to support peripheral nerve disease in practice, it was considered important to also assess the

suitability of 10% NBF as an alternative, since NBF is the fixative ubiquitously used in veterinary practices.

2.2.2 Fixation Protocol

PREPARATION OF ZAMBONI'S FIXATIVE

Prepared by Lynne Fleming, University of Glasgow.

125 ml of 16% paraformaldehyde stock solution was combined with 150 ml of saturated aqueous picric acid, made up to 1 l with 0.1 M phosphate-buffered saline (PBS) and adjusted to pH 7.3 by adding 10 M sodium hydroxide, dropwise (Bio-Rad, 2019; Stefanini et al., 1967).

PREPARATION OF 10% NEUTRAL BUFFERED FORMALIN

Prepared by post mortem room technical staff, University of Glasgow.

87.5 g of sodium dihydrogen phosphate, 162.5 g of di-sodium hydrogen phosphate and 2.5 l of formaldehyde were added to 2 l of distilled water, allowed to fully dissolve and made up to 25 l with distilled water.

SAMPLE FIXATION

For each animal, one biopsy sample from each site (proximal and distal) was placed in 1.5 ml of 10% NBF and the remaining two in 1.5 ml of Zamboni's fixative. All four samples were fixed at 4 °C and approximate fixation time was recorded (see Appendix B). Samples were then washed in 5 ml PBS for 5 minutes, placed in 30% sucrose in PBS (cryoprotectant) at 4 °C until they sank and stored for up to 24 hours. Following their retrieval from the cryoprotectant, samples were patted dry with paper towel and where necessary, hair was removed with small curved scissors (some animals were clipped by submitting veterinarians before sampling). Tissues were then placed in a cylindrical foil cryomould (8 mm diameter) and covered in optimal cutting temperature compound (OCT, Tissue-Tek® Sakura, Alphen aan den Rijn, The Netherlands) for 5 minutes, after which the cryomould was filled with OCT. Samples were orientated vertically (with the epidermis parallel to the long axis of the cryomould) and with the direction of hair growth parallel to the short axis of the

cryomould, immediately frozen on dry ice, sealed using Parafilm® M (Bermis Company, Neenah, Wisconsin, USA), labelled and stored at - 20 °C.

Sectioning

Tissue blocks were cut on a Leica CM1850 cryostat (Leica Biosystems, Nussloch, Germany) at – 22 ºC. Samples were placed in the cryostat 10 minutes before sectioning to acclimatise, then 50 µm sections were cut with the blade at an angle of 0º. The orientation of the tissue block to the blade was generally perpendicular to the epidermis and parallel to the direction of hair growth, however, for some tissues better sections were achieved with the blade parallel to the epidermis and cutting from the subcuticular aspect. Tissue blocks were cut until approximately 2 mm (for 3 mm biopsies – 2 dogs only) or 4 mm (for 6 mm biopsies – all remaining dogs) of epidermis was obtained per section. Consecutive sections were thaw mounted onto alternate plain glass slides (A and B series) so that examination of non-consecutive sections could be guaranteed. Three sections were mounted onto each slide and at least 4 slides per series were cut for each tissue block. Slides were examined using a microscope (x200 magnification) for quality of cutting and usable epidermis and were then placed immediately in a slide box on dry ice. Immunohistochemistry for each tissue block was carried out on the same day as blocks were cut and where repeats were required (due to handling damage to tissues) slides were stored for no longer than 6 days at - 20 ºC.

Slide preparation

Slides were thawed and dried at room temperature for 5 minutes. A barrier was created around each tissue section using an ImmEdge® Hydrophobic Barrier PAP Pen (Vector Laboratories, Burlingame, California, USA) and for the following steps the slides were placed on top of laminated black paper to aid visualisation of skin sections. OCT was removed by washing twice for 5 minutes with PBS. PBS washes were applied using a glass Pasteur pipette and during the second wash, the flow from the pipette was used

to gently lift the tissue section from the slide to ensure the section was free-floating in subsequent treatments.

Bleaching

The majority of tissue sections were not bleached due to the fragility of canine skin which necessitated keeping handling to a minimum. Necessity for bleaching was determined during quality control at the cutting stage by assessing three sections cut from each tissue block for density of melanin granules within the epidermis.

If tissue did require bleaching, 75 µl of 10% Hydrogen peroxide was added to each tissue section after the second PBS wash and sections were incubated at 37 °C for 3 hours in a moisture chamber. Hydrogen peroxide was removed, and sections were again washed twice with PBS for 5 minutes.

Immunohistochemistry

All incubations were performed with slides in a moisture chamber at room temperature and on a horizontal shaker at 70 rpm, and all solutions were applied at 75 µl per section. A maximum of 22 slides were processed in each immunohistochemistry (IHC) run.

Following slide preparation, and where necessary bleaching, PBS was removed, 3% hydrogen peroxide in methanol was applied and sections were incubated for 45 minutes. Two PBS washes of 5 minutes were applied and after PBS removal, sections were blocked with 1% normal horse serum (NHS) in PBS for 30 minutes. Excess serum was removed by pipette and a 1:10,000 dilution of anti-PGP 9.5 antibody (ab8189, Abcam, Cambridge, UK) with 2% NHS in 0.1% Tween-20/Tris buffered saline (TBST) was applied and sections were incubated overnight. Two PBS washes of 5 minutes were carried out and anti-mouse/rabbit secondary antibody (Vectastain Elite ABC universal kit, Vector Laboratories, Burlingame, California, USA), prepared according to manufacturer's instructions, was applied and sections were incubated for

1 hour. Tissue sections were then washed with PBS for ten minutes followed by two washes of 5 minutes. Vectastain enzyme reagents (Vectastain Elite ABC universal kit, Vector Laboratories, Burlingame, California, USA), prepared according to manufacturer's instructions, were applied and incubated for 1 hour. Distilled water was then used to wash sections twice for 5 minutes. Vector SG chromogen (Vector Laboratories, Burlingame, California, USA), prepared according to manufacturer's instructions, was applied for 12 minutes, followed by removal and immediate application of Vector Hematoxylin QS (Vector Laboratories, Burlingame, California, USA) diluted to 1:30 with distilled water. After 4 minutes, sections were washed twice with distilled water for 30 seconds. Excess water was removed by pipette and slides were mounted as soon as sections appeared dry.

Figure 2.3 Slides undergoing immunohistochemical staining on a shaker and in a moisture chamber.

Mounting

Sections were mounted and coverslipped with polyvinylpyrrolidone aqueous mounting medium.

For this, polyvinylpyrrolidone of molecular weight 10,000 (25 g) was dissolved in 25 ml of distilled water on a magnetic stirrer over several hours. 1 ml of glycerol and one small crystal of thymol were added (Kiernan, 1999).

Mounted slides were stored at room temperature.

Epidermal Measurement

The length of usable epidermis for each tissue section was measured using an Olympus BX51 microscope with an Olympus DP71 camera and Olympus software Stream (version 1.9.2) at x 20 magnification. Epidermal length was measured at its superficial surface and with apparent follicular epidermis, folded or damaged regions, and epidermis completely detached from any underlying dermis excluded. Images with embedded measurements were saved for each section to enable counting of measured regions only (Figure 2.4).

Figure 2.4 Examples of measurement of epidermal length, for IENF quantification.

For each skin sample, the aim was to produce a length of epidermis totalling at least 20 mm suitable for fibre quantification, and to include at least 3 tissue sections from the same series in the quantification. Where this was not achieved during the initial IHC run, further slides were subjected to IHC.

IENF Quantification

IENF quantification was performed using Olympus BX51 microscopes at x600 magnification (brightfield) and additionally using x400 magnification where this aided clarification of the course of fibres.

Two separate counting protocols were used. Protocol 1 represented a published protocol used for IENF counts on human skin (Mangus et al., 2019). However, since commonly the exact extension of the basal cell layer was not apparent in the sections under investigation, also an amended counting protocol (Protocol 2) was used which corresponded to that described by Kennedy et al. (2005) and reiterated in the guidelines of the European Federation of Neurological Societies (Lauria et al., 2005a).

2.10.1 Protocol 1

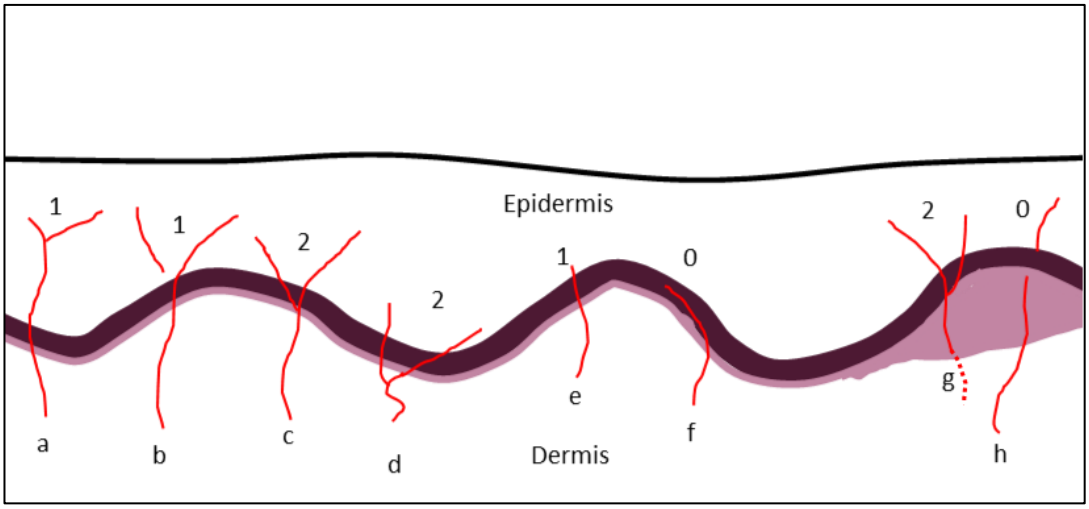

Figure 2.5 Line diagram depicting the IENF counting rules for Protocol 1.
Adapted from Mangus et al., (2019).
Black line; epidermal surface. Dark purple; basal cell layer of epidermis. Light purple; basement membrane. Red; IENF. (a, b) Nerve fibres were counted as they crossed the basement membrane (BM) of the epidermis. (c) Nerves that branched at the BM and entered the basal cell layer were counted as separate units. (d) Nerves that split below the BM were counted as separate units. (e) Nerve fragments that crossed the BM and passed vertically a single layer of the basal keratinocytes were counted. (f) Nerve fibres that approached the BM but did not cross the basal keratinocyte were not counted. (g) Nerves that branched within the basal cell layer were

counted separately. When the BM shifts at different planes only the epidermal axons that have continuous connection with the dermal axons were counted. (h) Epidermal axons that had no continuous connection with the dermal axons were not counted (Mangus et al., 2019).

2.10.2 Protocol 2

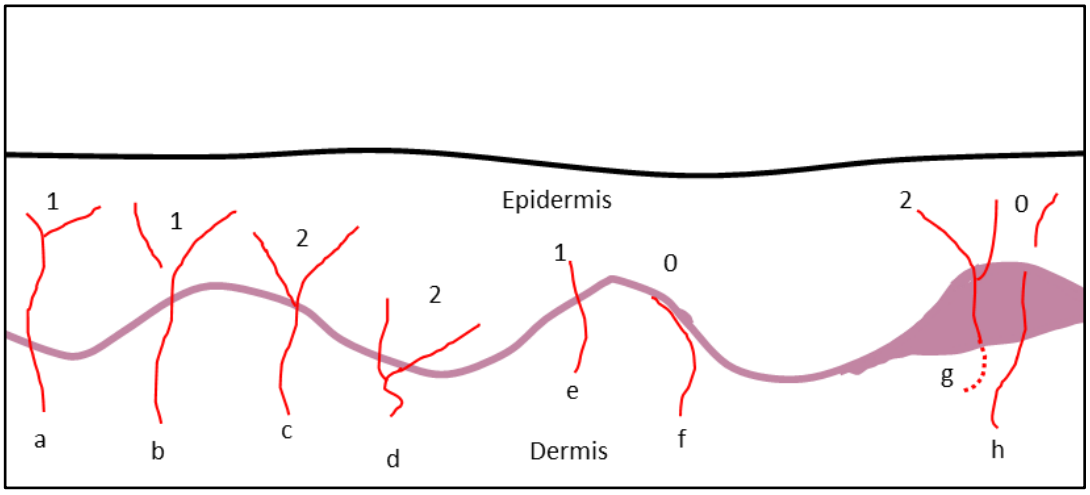

Figure 2.6 Line diagram depicting the IENF counting rules for Protocol 2.
Adapted from Mangus et al., (2019) and Kennedy et al., (2005).
Black line; epidermal surface. Light purple; basement membrane. Red; IENF. (a, b) Nerve fibres were counted as they crossed the basement membrane (BM) of the epidermis. (c) Nerves that branched at the BM were counted as separate units. (d) Nerves that split below the BM were counted as separate units. (e) Nerve fragments that crossed the BM were counted. (f) Nerve fibres that approached the BM but did not cross were not counted. (g) When the BM shifts at different planes only the epidermal axons that have continuous connection with the dermal axons were counted. (h) Epidermal axons that had no continuous connection with the dermal axons were not counted (Kennedy et al., 2005).

Repeatability

Test-test reliability or repeatability refers to the reproducibility of values of a test or of measurement in repeated trials on the same individuals. To assess the reproducibility of IEFND (fibres/mm) produced by the methods used in this study both intra-observer and inter-observer (2 observers) reproducibility were investigated. Additionally, Observer 1 also assessed the intra-sample reproducibility on two separate section series (A and B series) from the same skin biopsy and for both fixatives (both samples being from the same body region). Zamboni-fixed samples (designated reference samples due to representing the recommended fixative in human protocols) were used to assess the intra-observer and inter-observer reproducibility. All reliability analyses were carried out for both quantification protocols. Observers were not blinded to the identification for each section, however, all counts were carried out oblivious to previous results.

Statistical Analysis

Except where stated, all statistical analyses were carried out using the statistical programming language R (R Core Team, 2019). For analysis of independent variables and their influence on IENFD, the Brown-Forsythe test (levene.test, lawstat package (Lyubchich et al., 2019)) for homogeneity of variance was applied to assess the appropriateness of applying one-way ANOVA (aov, base R). The Anderson-Darling test for normality (ad.test, nortest package (Gross and Ligges, 2015)) was applied to assess the normality of distribution of differences before applying paired t-tests (t.test, paired = TRUE, base R). For multiple linear regression (lm, base R) stepwise model fitting was performed using the stepAIC function in the MASS package (Ripley and Venables, 2002).

Repeatability analyses were carried out according to the methods of Bland and Altman (Bland and Altman, 1999, 1986). The confidence interval of the bias was calculated using the package 'blandr' (Datta, 2017). Confidence intervals for the repeatability coefficient (RC) were calculated according to Barnhart and Barboriak, (2009) using *R code provided by Ian Graham, Liverpool Football Club.* Additionally, where appropriate, standard error of the measure (SEM) (Weir, 2005) also known as typical error (TE) and coefficient of variation (Hopkins, 2000) were calculated. Calculation of SEM was undertaken using the package 'rel' (LoMartire, 2020) in R. Confidence limits for the coefficient of variation were calculated using a spreadsheet provided by Hopkins (Hopkins, 2007, 2000). For comparison of methods using replicates, the package 'MethComp' (Carstensen et al., 2020) was used to produce limits of agreement (LoA) using a simple model (unpaired replicates). Differences on averages regression (DA.reg, MethComp) and differences versus averages plots were used to confirm whether logarithmic transformation of data was appropriate. For selected comparisons with published studies, intra-class correlation was performed using the 'irr' package (Gamer et al., 2012) in R, with a two-way model of type 'agreement'.

3. RESULTS

Sample Information

3.1.1 Signalment and History

Samples from 45 canine cadavers were obtained, 36 of which were submitted with signalment and clinical history. Signalment and history are summarised in Table l.1 and further information for all dogs including fixation times, body condition scores (BCS) and PMI are included in Appendix B.

For 36 animals, the age in years or months was reported. Of the remaining 9 dogs, 5 were described as adult and 4 as geriatric. Dogs were split into age groups, comprising juveniles (0-18 months; n=4), adults (18 months-10 years; n=31) and geriatrics (> 10 years; n=10). There were 4 Staffordshire bull Terriers, 3 German shepherd dogs and 3 Labradors. All remaining dogs represented a single dog of that particular breed. Of the 29 animals which were body condition scored, 24 had a good BCS (2-3/5). The sex ratio of animals was relatively even; 10 female entire, 10 female neutered, 12 male entire and 13 male neutered dogs.

Seven of the 45 dogs had neurological signs, however, in all dogs these were reported to originate from the central nervous system with diagnoses including underlying degenerative myelopathy (dog 66), brain and spinal cord masses (dogs 74, 82, 83), suspicion of infection with canine distemper (dog 73), congenital generalised osteodystrophy and pathological fractures including of the dens axis (dog 27), whilst one dog had acute onset CNS signs which were not otherwise described (dog 75, later excluded from analysis). Since the case with degenerative myelopathy was surmised to potentially exhibit changes to the peripheral nervous system, this case was processed purely for interest and excluded from analyses.

3.1.2 Samples used for Analysis

Only 3 dogs (43, 75, 76) produced tissue sections which all required bleaching, of which two (43 and 75) could not be processed successfully despite several attempts. This was due to fragility and thinness of the skin of a Lurcher (dog 43) and due to very high follicular density in a Labrador (dog 75), in turn again resulting in very fragile skin sections. One other dog (a Terrier cross, dog 40), with thin skin could also not be processed, which meant that 3 dogs were excluded from the study at this point (dogs

40, 43 and 75). The mean number of sections required to produce 20 mm of usable epidermis for each sample was 5.12.

Of the four skin biopsies from each of the remaining 41 dogs (the case with degenerative myelopathy being excluded), Zamboni's fixed samples taken from the proximal site (ZT) were chosen as the reference set due to Zamboni's fixative being one of the recommended fixatives and the proximal site was expected to have a higher IENFD compared to distal. Overall, 6/41 tissue sets were rejected from further analysis due to the lack of available tissue (dog 31), due to large amounts of melanin (in the ZT sections specifically) which was not sufficiently reduced by bleaching (dogs 28 and 65), or due to persistent variation in nerve fibre chromogen uptake which could not be rectified by processing newly cut sections (dogs 24, 25 and 29). Ultimately and excluding the dog with degenerative myelopathy, 35 dogs were included in the quantification of IENF in ZT tissues.

For Zamboni's fixed samples from the distal site (ZB), 5/41 samples (dogs 28, 30, 53, 54, 70) (again excluding the degenerative myopathy case) were rejected as it was not possible to produce 20 mm of epidermis suitable for IENF quantification. For 7/36 successfully processed samples (dogs, 57, 58, 67, 69, 80, 82, 83) IENF quantification was not possible due to external factors creating unforeseen and immediate time constraints (COVID-19 lockdown). Therefore, in total 29 animals were included for quantification of IENF in ZB tissues.

To investigate intra-sample reproducibility of IENF quantification, two separate sets of slides comprising alternating skin sections (A and B series) each for one Zamboni's fixed sample and one formalin-fixed sample were processed and measured for the last 10 dogs entering the study (dogs 04, 44, 50, 70, 71, 72, 73, 74, 76, 87). For one of these animals (dog 76) it was not possible to produce 20 mm of suitable epidermis for quantification of the formalin samples due to persistent variability in chromogen uptake.

Apart from the 9 above-mentioned formalin-fixed samples, 3 other biopsy samples fixed in formalin were processed and underwent quantification; two from the distal site (dog 81 FB and dog 83 FB) and one from the proximal site (dog 81 FT). Therefore, a total of 10 FT samples and 11 FB samples were available for analysis.

Dog number	Breed	Age	Sex	History / Diagnosis
4	labrador	10 years	FE	Mediastinal lymphoma
10	wheaten Terrier	10 years	MN	Prostate mass
16	samoyed	4 years	MN	Pleural effusion
21	greyhound	Geriatric	MN	Incontinence
24	English bulldog	2 years	FN	Hyperthermia
25	Yorkshire terrier	Geriatric	FE	-
26	lhasa apso	Geriatric	FN	Pituitary and adrenal enlargement
27	pomeranian	5 months	ME	Fracture of the dens, CNS signs
28	poodle cross	1 year	FE	-
29	German shepherd dog	3 years	FE	Pulmonary bullae rupture
30	West Highland white terrier	13 years	MN	Neoplasia
31	American bulldog	5 months	ME	Gastric dilatation-volvulus
32	beagle	8 years	ME	Mammary tumour
33	German shepherd dog	8 years	ME	Haemangiosarcoma
34	cocker spaniel x poodle	5 years	MN	Inflammatory bowel disease
35	labrador x poodle	8 years	FN	Acute hepatopathy
38	springer spaniel	13 years	FE	-
40	*terrier cross*	*Geriatric*	*FN*	-
43	*lurcher*	*11 years*	*FN*	-
44	crossbreed	8-10 years	FE	Pyometra
46	Border collie	4 years	MN	-
48	American bulldog	4 years	FE	-
50	American cocker spaniel	Adult	ME	-
52	Staffordshire bull terrier	Adult	ME	Arthritis
53	Staffordshire bull terrier	9 years	FE	Mammary masses
54	rough collie	4 years	ME	Hip dysplasia
55	Staffordshire bull terrier	4 years	FN	Vomiting
57	Staffordshire bull terrier	4 years	MN	-
58	Border Collie Cross	Adult	ME	Cardiomegaly
65	doberman	8 years	MN	Lymphoma
66	*German shepherd dog*	*9 years*	*FN*	*Degenerative myelopathy*
67	golden retriever	4 years	FN	Sudden death
69	papillon	2 years	MN	Sudden death
70	collie cross	11 years	ME	-
71	labrador cross	8 years	ME	Liver failure
72	miniature schnauzer	9 years	FE	Disseminated bleeding
73	Patterdale terrier	3 months	ME	Seizures (infectious origin suspected)
74	cairn terrier	11 years	MN	T4 spinal cord mass, paraplegia
75	*labrador*	*11 years*	*MN*	*Acute onset CNS signs*
76	English bulldog	2 years	ME	Sudden death (respiratory arrest?)
80	labrador	Adult	MN	Sudden death
81	Tibetan terrier	5 years	FN	Suspected cholangiocarcinoma
82	boxer	8 years	MN	Suspected meningioma
83	miniature schnauzer	6 years	FN	Extradural mass T1-T2
87	dogue de Bordeaux	Adult	FE	Orthopaedic

Table l.1 Signalment and clinical history/post mortem diagnosis of animals sampled. Italics - rejected animals.

For 2 dogs, the fixation time of samples was 16 hours (dogs 16 and 21), however samples were difficult to cut (see Appendix C) and fixation times (see Appendix B) were extended to at least 64 hours for Zamboni's-fixed samples (median 64 hours; maximum 136 hours) and 40 hours for formalin-fixed samples (median 64 hours; maximum 136 hours).

Intraepidermal Nerve Fibre Density

The results for IENFD of Zamboni's fixed samples from the proximal site (ZT; n=35), assessing ≥20 mm per animal and using both protocols, were right-skewed with a median of 1.90 fibres/mm for Protocol 1 (mean 2.60 fibres/mm) and 2.45 fibres/mm for Protocol 2 (mean 3.10 fibres/mm). For each data set in this study, Protocol 2 gave consistently higher (and more reproducible) IENFD results, therefore, these will be discussed in more detail in this text. The minimum IENFD (≥20 mm epidermis) was 0.66 fibres/mm and the maximum was 10.89 fibres/mm. Summary statistics for IEFND of ZT samples are presented in Table 3.2 and individual count data in Figure 3.6.

Statistic	Protocol 1	Protocol 2
Minimum	0.43	0.66
Maximum	9.21	10.89
Median	1.90	2.45
Mean	2.60	3.10
1st quartile / 3rd quartile	1.44 / 3.37	1.80 / 3.90
Lower 5th percentile	0.53	0.77

Table 3.2 Summary statistics for IENFD per dog (all ages) assessing ZT samples (n=35; values represented in fibres/mm).
For samples which also contributed to repeatability analysis, the mean IENF density of both counts obtained by Observer 1 was used. The lower 5th percentile is recommended as a clinical cut-off point in human studies. For reference intervals derived from less than 40 subjects some authors recommend using the minimum measured value as a cut-off (Latimer, 2011). Upper and lower quartile ranges are given in preference to standard deviation for skewed data.

Since neurological cases were included, and also because a 3 month old dog represented an outlier with an IENFD of 10.89 fibres/mm for Protocol 2, the analysis was repeated excluding all neurological cases and juvenile animals (0-18 months old). This yielded a median of 2.45 fibres/mm (mean 3.10 fibres/mm) for Protocol 2 (Table 3.3), however, importantly, the minimum IENFD and lower 5th percentiles were unchanged after removing neurological cases and juveniles.

Statistic	Protocol 1	Protocol 2
Minimum	0.43	0.66
Maximum	6.19	6.67
Median	1.89	2.31
Mean	2.37	2.83
1st quartile / 3rd quartile	1.41 / 3.25	1.76 / 3.74
Lower 5th percentile	0.53	0.77

Table 3.3 Summary statistics for IENFD of ZT samples with juveniles and neurological cases removed (n=30; values represented in fibres/mm).
For samples which also contributed to repeatability analysis, the mean IENF density of both counts obtained by Observer 1 was used. The lower 5th percentile is recommended as a clinical cut-off point in human studies. For reference intervals derived from less than 40 subjects some authors recommend using the minimum measured value as a cut-off (Latimer, 2011). Upper and lower quartile ranges are given in preference to standard deviation for skewed data.

For analysis of effects of dog and sample characteristics upon IENFD, results for counts according to Protocol 2 by Observer 1 are reported. All analyses were repeated on the data set with neurological cases and juveniles removed and the results were unchanged.

3.2.1 Effect of Dog Characteristics on IENFD

Effect of Sex on IENFD

Of the 35 ZT samples in this dataset, 7 were from female entire (FE), 6 from female neutered (FN), 11 from male entire (ME) and 11 from male neutered (MN) animals. IENFD grouped by sex are presented in Figure 3.1.

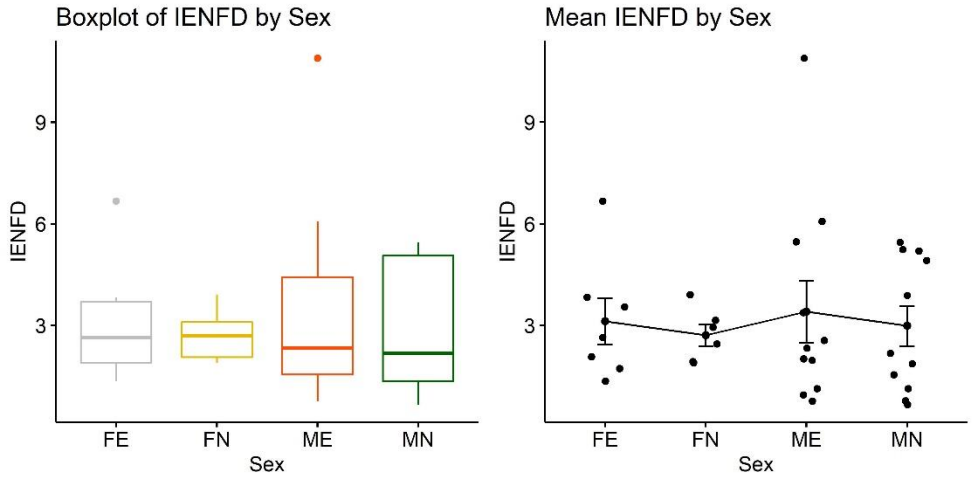

Figure 3.1 IENFD by sex (Observer 1, ZT; n=35).
FE – female entire, FN – female neutered, ME – male entire, MN – male neutered.

Since there was no significant difference in group variances (Brown-Forsythe test for homogeneity of variance, P-value: 0.441), data were subjected to one-way analysis of variance (ANOVA), rather than the non-parametric equivalent. There was no significant difference in group means (P-value: 0.933). Analysis was repeated for the

groups male and female Figure 3.2 and again there was no significant difference in group variances (P-value: 0.140) or group means (P-value: 0.727).

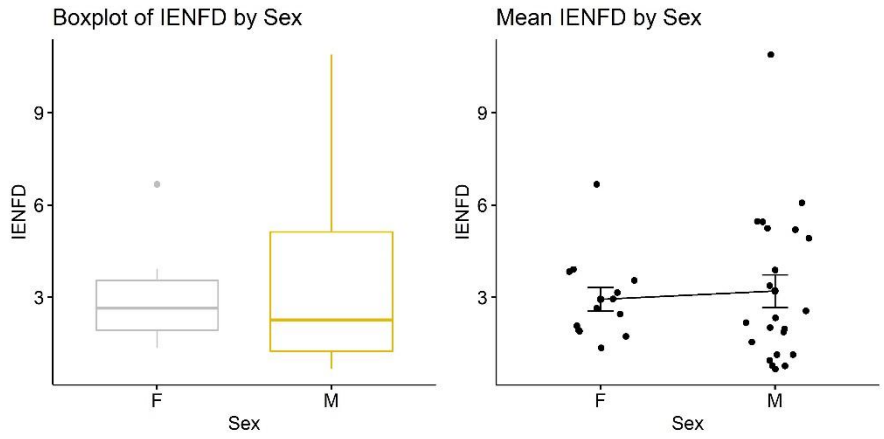

Figure 3.2 IENFD by sex (Observer 1, ZT; n=35).
F – female, M – male.

Effect of Age on IENFD

For the 35 ZT samples quantified, the juvenile age group (0-18 months) comprised 2 dogs, the adult age group (18 months -10 years) 27 dogs, and the geriatric age group (> 10 years old) 6 dogs. The Brown-Forsythe test for homogeneity of variance gave a P-value of 0.009 for the IENFD for these three groups, therefore ANOVA was not performed.

Analysis was repeated, dividing adults into young adult (18 months - 5 years) and adult (>5 years old < 10 years), yielding 11 young adults and 16 adults after which, the Brown-Forsythe test still produced a P-value < 0.05 (0.02). Therefore, as there were only 2 subjects, juvenile animals were, again, removed from the analysis (Figure 3.3). Thereafter, the Brown-Forsythe test returned a P-value of 0.691, and one-way ANOVA was performed (P-value: 0.395), giving no evidence of a significant difference in IENFD grouped by age. Linear regression supported that the null hypothesis of juvenile age having no effect on IENFD could not be rejected (coefficient P-value: 0.03). However, since the juvenile group included only 2 subjects, one of which one was considered an outlier, no definite conclusions could be drawn.

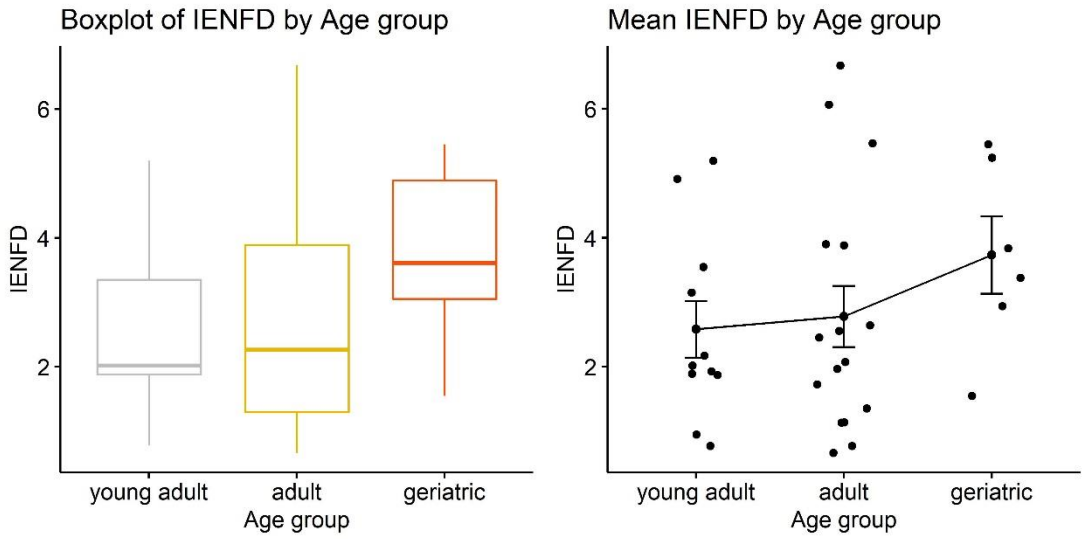

Figure 3.3 IENFD by age group (Observer 1, ZT; n=33).

3.2.2 Effect of site on IENFD

The data obtained with Protocol 2 also were used to perform a paired t-test in order to detect differences in IENFD of each dog depending on whether proximal or distal site were assessed. Twenty-four pairs of samples were available and plots of these data are presented in Figure 3.4. The Anderson-Darling test for normality returned a P-value of 0.246, and the P-value for the paired t-test was 0.780. Therefore, the null hypothesis that IENFD was the same for proximal and distal sites could not be rejected.

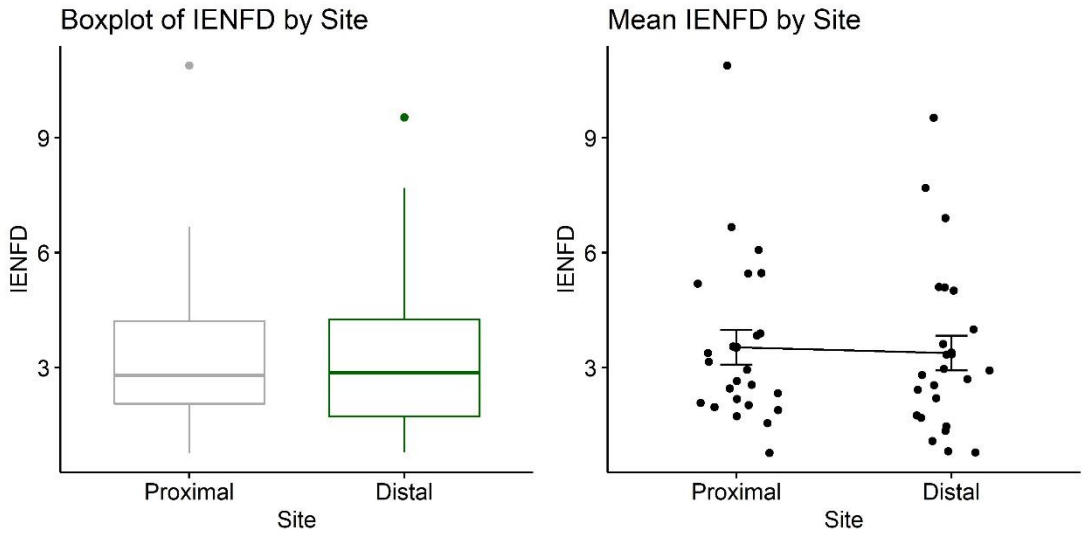

Figure 3.4 IENFD by site (Observer 1, Zamboni's fixed; n=24).

3.2.3 Effect of fixative on IENFD

Due to the small number of formalin-fixed samples quantified (n=21) and the smaller number of these for which paired Zamboni's-fixed samples were available (n=13), proximal and distal sites were analysed together. For Zamboni's-fixed samples which underwent recounting, the mean IENFD obtained from both counts was used in this analysis. Plots of these data are presented in Figure 3.5. The Anderson-Darling test produced a P-value of 0.016, so a Wilcoxon signed-rank test was performed and produced a P-value of 0.684 indicating that there is no significant difference in IENFD for Zamboni's-fixed samples when compared to formalin-fixed samples.

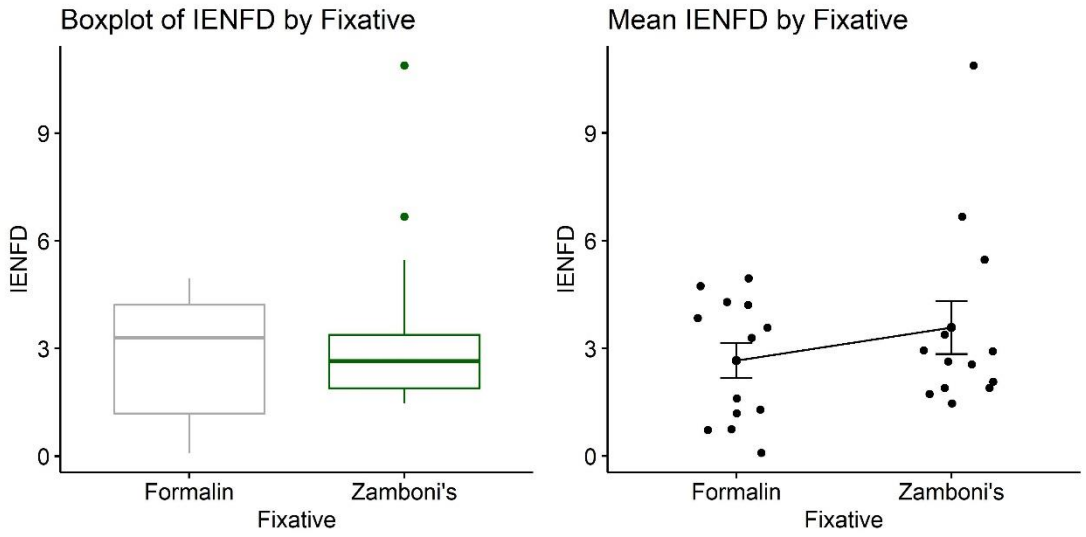

Figure 3.5 IENFD by fixative (Observer 1; n=13).

3.2.4 Effect of other variables on IENFD

Body condition score, post mortem interval and fixation time were plotted against IENFD and no relationship was identified between any of these independent variables and IENFD. For completeness, a multiple regression model fit using a stepwise approach was attempted using all variables for which there was a complete data set (age group, sex, PMI and fixation time). These variables do not predict IENFD, either using 4 categories for sex (FE, FN, ME, MN; F (7, 27) = 0.152, P-value: 0.992, R^2: 0.038), nor using 2 categories for sex (F, M; F (5, 29), P-Value: 0.983, R^2: 0.023).

Repeatability

3.3.1 Intra-observer repeatability

For Observer 1, intra-observer repeatability was investigated both for the full ≥20 mm length of epidermis available for each sample and also for ≥9 mm of epidermis and a minimum of 3 sections per sample. For Observer 2, intra-observer repeatability was only investigated for ≥9 mm of epidermis and a minimum of 3 sections per sample.

OBSERVER 1 – ≥20 MM LENGTH OF EPIDERMIS

Thirty Zamboni's-fixed samples were used. Each tissue section was subjected to IENF counting twice and the second count took place at least 4 days after the first. The mean length quantified was 22.05 mm. Results are shown in Figure 3.6 and suggest a slightly better correlation between counts for Protocol 2 than for Protocol 1.

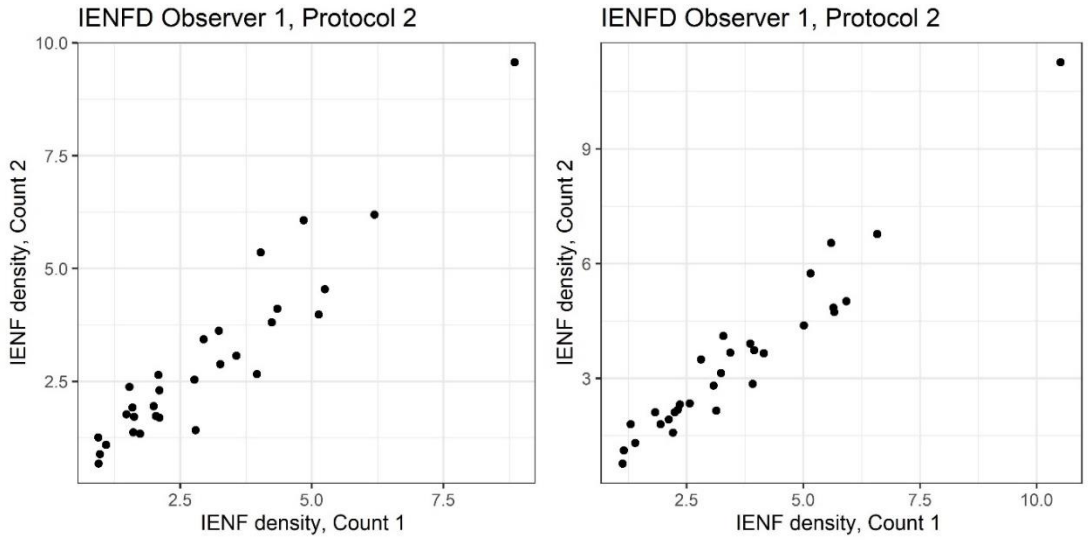

Figure 3.6 IENFD (fibres/mm) quantification recounts for Observer 1 (ZT, 20 mm).

BLAND-ALTMAN ANALYSIS

The repeatability coefficient (RC) represents the value below which the difference between any two repeated measurements may be expected to lie with a probability of 95%, calculated as 1.96 times standard deviation of the differences (SD_d) (Bland and Altman, 1986). Calculation of RC by this method is appropriate if (1) the bias of differences (which corresponds to mean difference in untransformed datasets) is not significantly different from zero, (2) the individual differences (difference scores) are normally distributed and (3) difference scores do not rise significantly with mean

(otherwise RC will be overestimated). The RC (on untransformed data) is given in the same units as the measurement (fibres/mm). A low RC indicates better reproducibility than a high RC.

In this data set, diagnostic plots confirmed that zero fell within the 95% confidence interval for the bias of differences (Figure 3.7), meaning that there was no significant systematic difference between count 1 and count 2 and therefore assumption (1) above was not violated. Statistics for repeatability for Observer 1 are given in Table 3.4. The plots revealed an increase in the difference scores (individual differences between 2 replicates) with increased means particularly for Protocol 2 (Figure 3.7), meaning that assumption (3) above may have been violated. This is clearer when viewing (absolute) differences versus averages (means) plots (Carstensen et al., 2020) (Figure 3.8). Since the RC assumes that the bias of differences is zero, and it is given as an absolute number in the same units as the measurement (Table 3.4), it is not illustrated in plots in this text, to avoid confusion with (asymmetrical) limits of agreement, which are relevant to agreement between methods and not to intra-observer repeatability.

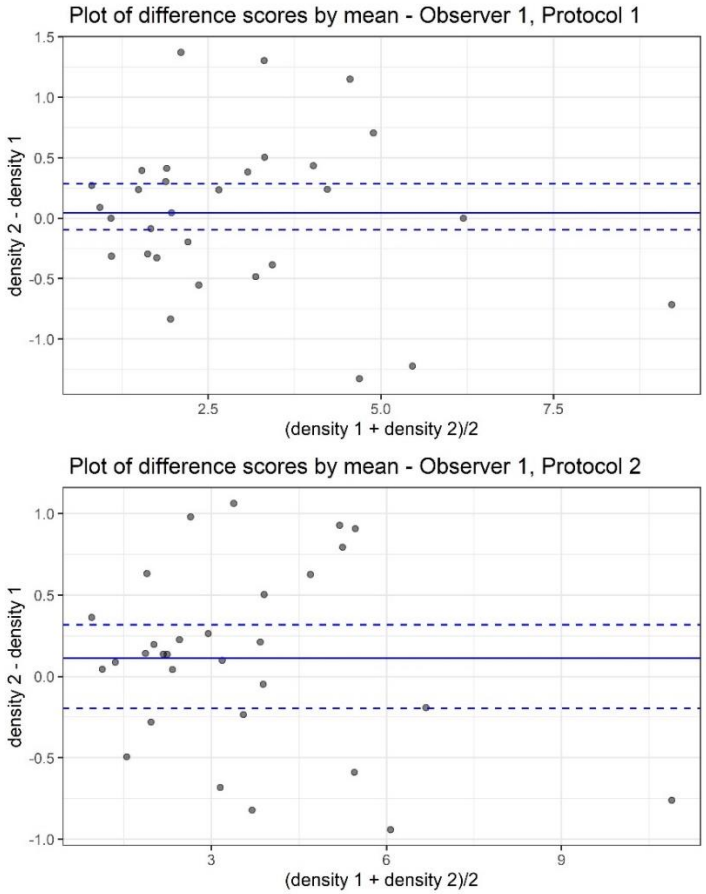

Figure 3.7 Difference scores by means plots for Observer 1 (ZT, 20 mm).
Continuous line – bias of differences (mean difference). Dashed line – 95% CI of bias of differences.

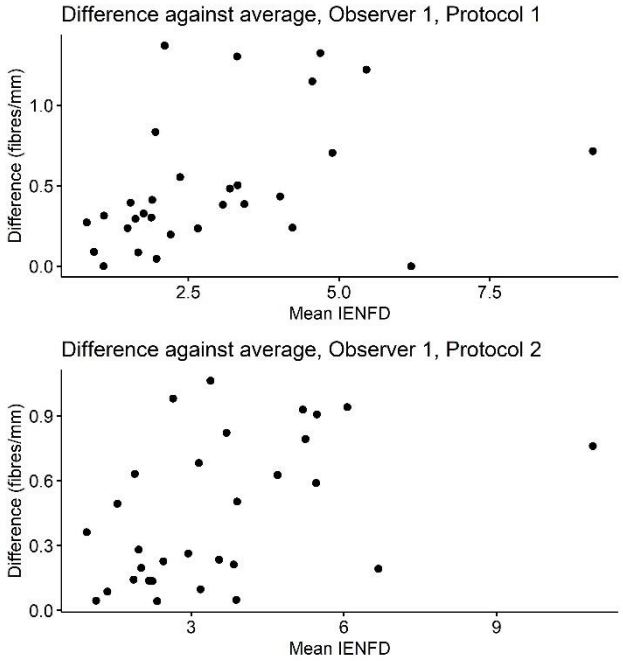

Figure 3.8 Intra-observer differences against averages plots for Observer 1 (ZT, 20 mm).

When difference scores rise with the mean (as in this case), Bland-Altman analysis of untransformed data will tend to overestimate the repeatability coefficient for test results with lower values (and those lower values in turn are considered the most important in the diagnostic application of IENF quantification). Here, the logarithmic transformation is recommended (over other transformations), because the output can be related to the actual test values. The geometric mean ratio of the replicate values is reported instead of the mean difference, and the RC can be expressed as a percentage of the measurement (see interpretation below).

In this case, differences on averages regression indicated that the null hypotheses of constant differences between methods (P-value Protocol 1: 0.589; P-value Protocol 2: 0.378) and constant residual variance (P-value Protocol 1: 0.290; P-value Protocol 2: 0.378) with the logarithmic transformation could not be rejected, thus log-transformed plots showing a more constant variance with mean IENFD are presented in Figure 3.9. The Shapiro-Wilks test for normal distribution of the difference scores produced a P-value of 0.641 for Protocol 1 and 0.376 for Protocol 2 for untransformed data, and 0.812 and 0.542 respectively for log transformed data, therefore 95% confidence intervals (CIs) for the RC could be calculated for either condition.

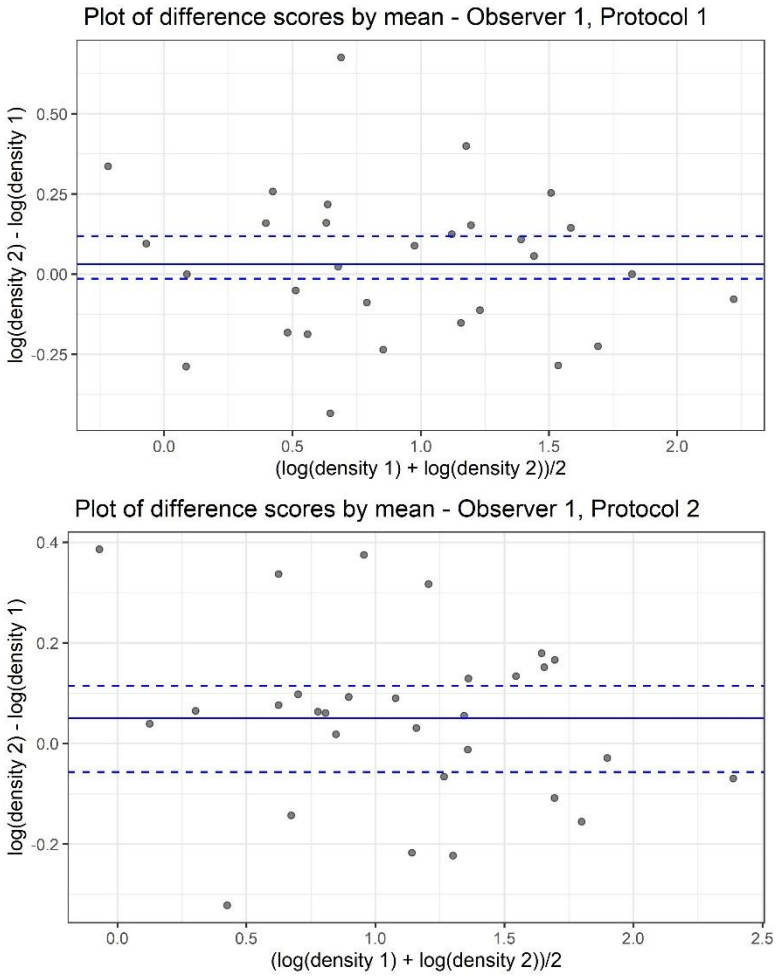

Figure 3.9 Difference scores by means plots (log transformed data) for Observer 1 (ZT, 20 mm). Continuous line – bias of differences. Dashed line – 95% CI of bias of differences. Density – IENFD.

Logarithmic transformation of both density measurements was applied, and the mean difference and repeatability coefficient were back-transformed to produce the geometric mean ratio and the RC as a ratio respectively (Table 3.4).

Statistic	Protocol 1	Protocol 2
Mean Difference (fibres/mm)	0.04	0.11
Standard deviation of differences	0.65	0.55
Repeatability coefficient (fibres/mm) (95% CI)	1.27 (1.01 – 1.69)	1.08 (0.87 – 1.45)
Geometric Mean Ratio	1.03	1.05
Log density SD_d	0.235	0.172
Log density RC as ratio (95% CI)	1.585 (1.445 – 1.851)	1.401 (1.310 – 1.571)
Log density RC % (95% CI)	58.5 (44.5 – 85.1)	40.1 (31.0 – 57.1)

Table 3.4 Bland-Altman repeatability statistics for Observer 1 (ZT, 20 mm).

However, examination of Figure 3.7 and Figure 3.8 also suggested that for higher mean fibre densities, the proportional increase in variance was not linear and with rising mean values the proportional increase reduced (or even plateaued), meaning that the logarithmic transformation could have underestimated the repeatability coefficient at

lower values and overestimated at higher values. In order to investigate whether this overestimation was likely to be clinically relevant and since this study is most concerned about samples with low IENFD (in order to differentiate normal from diseased samples) the analysis was repeated on the 15 samples with mean density below 3 fibres/mm. This cut-off was based on diagnostic plots (not shown) indicating the samples for which logarithmic transformation produced the best fit. Results are presented in Table 3.5.

Statistic	Protocol 1	Protocol 2
Geometric Mean Ratio	1.03	1.10
Log density SD_d	0.191	0.186
Log density RC as ratio (95% CI)	1.715 (1.539 – 2.058)	1.456 (1.351 – 1.653)
Log density RC % (95% CI)	71.5 (53.9 – 105.5)	45.6 (35.1 – 65.3)

Table 3.5 Bland-Altman repeatability statistics for samples with mean fibre density <3fibres/mm for Observer 1 (ZT, 20 mm).

Summarising the results, the repeatability coefficient for the complete data set when assessing untransformed data was 1.27 fibres/mm for Protocol 1 and 1.08 fibres/mm for Protocol 2, whilst when assessing log-transformed data, was 58.5% and 40.1%, respectively. For the data set comprising samples with low means, the repeatability coefficient was 71.5% (95% CI: 53.9-105.5%) for Protocol 1 and 45.6% (95% CI: 35.1 – 65.3%) for Protocol 2.

Other Repeatability Measures

An alternative method of quantifying test-retest reliability is estimation of standard error of the measure (SEM) (Weir, 2005) also known as 'typical error' (TE) (Hopkins, 2000). Weir recommends derivation of the "minimum difference to be considered real" (MD) (which equals the Bland-Altman coefficient of repeatability (repeatability coefficient), Table 3.4), from the SEM. Coefficient of variation (CV) is the typical error expressed as a percentage of the measurement mean. To investigate repeatability considering increasing difference scores with mean, logarithmic transformation of IENFD was performed (for which typical percentage error equals typical error of log-transformed data multiplied by 100). For log transformed data with errors >5%, asymmetric typical errors were calculated where variation about the mean is 1/(1+ estimate) to 1+ estimate (Hopkins, 2000). The results are presented in Table 3.6. Comparison of the CVs (obtained from non-transformed data) with the typical error estimates produced by log transformation allows a subjective assessment of the effect of the log transformation. In the case of these data sets, these CVs and TE estimates

were similar indicating that 'best fit' for these data sets lay between log transformation and no transformation, as previously discussed.

Statistic	Protocol 1	Protocol 2
SEM / TE (fibres/mm)	0.46	0.39
Coefficient of variation % (0.95 CI)	15.45 (12.75 – 19.77)	11.08 (9.15 – 14.18)
Typical percentage error estimate (Log density)	16.6	12.2
Typical error – reduction in measure % (90% CI)	14.2 (11.7 – 18.2)	10.9 (9.0 – 14.0)
Typical error – increase in measure % (90% CI)	16.6 (13.7 – 21.2)	12.2 (10.1 – 15.6)

Table 3.6 Intra-observer typical error, Observer 1 (ZT, 20 mm).

Additionally, intra-observer correlation was calculated for Protocol 2 to be able to compare the results with published studies on human skin (ICC 0.96, 95% CI; 0.92 – 0.98, F (29,30): 56, P-value: <0.001).

INTERPRETATION

For the protocol with better repeatability (Protocol 2), the repeatability coefficient (using the whole data set, with log transformation) was 40.1%. If we considered the lower 5th percentile of nerve fibre density derived previously (section 3.2) for Protocol 2 by Observer 1 (0.77 fibre / mm) then the maximum measured IENFD for which we could be 95% confident repeat quantification would fall below the lower 5th percentile would be 0.55 fibres/mm (0.77 ÷ 1.401). If we used the minimum IENFD as cut-off then the maximum measured IENFD for which we could be 95% confident repeat quantification would fall below the cut-off would be 0.47 fibres/mm (0.66 ÷ 1.401). For a sample size of less than 40 (as in this study), using the minimum measured value to produce a reference interval is recommended (Latimer, 2011).

Applying the results acquired to the data set with low mean densities, the maximum measured IENFD for which we could be 95% confident repeat quantification would fall beyond the 5th percentile would be 0.53 fibres/mm (0.77 ÷ 1.456) and using the minimum IENFD would be 0.45 (0.66 ÷ 1.456) fibres/mm.

The difference between results for the complete data set and data set only using low means, equated to a difference between 11 and 10.6 or 9.4 and 9 fibres in 20 mm of epidermis (depending on which cut-off is used), and is unlikely to be of clinical significance. Therefore, the repeatability coefficient based on log transformed data

appears clinically valid, as analysing the whole data set did not produce a clinically relevant under-estimation of the RC.

OBSERVER 1 – ≥9 MM LENGTH OF EPIDERMIS

The first 3 recorded sections were selected from each sample and, where necessary, supplemented by further sections, to provide at least 9 mm of measured epidermis for analysis of test-test reliability for Observer 1 for ≥9 mm and compare this with the results obtained from the ≥20 mm quantification described above. Mean length quantified was 13.51 mm. Results are shown in Figure 3.10.

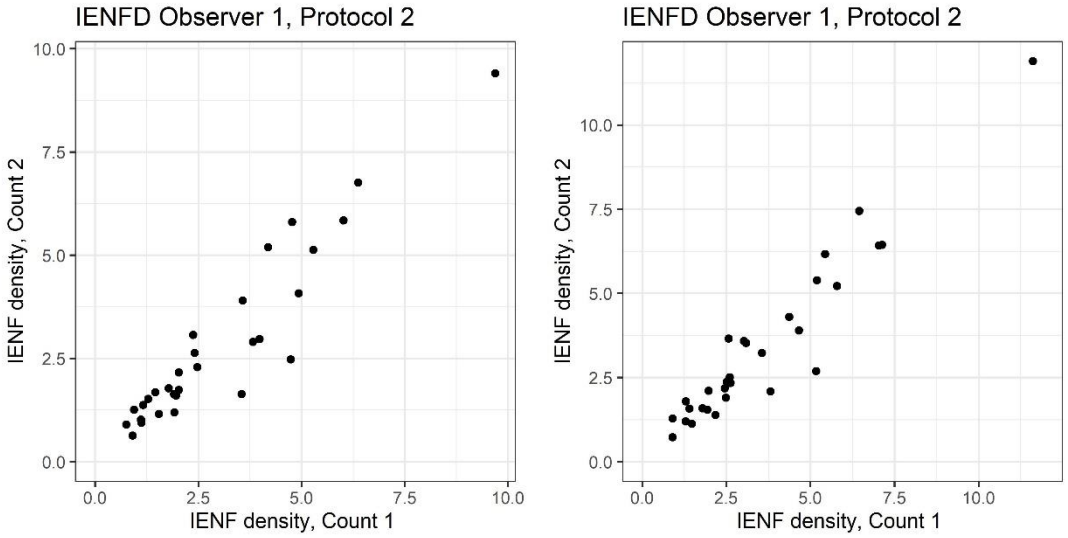

Figure 3.10 IENFD (fibres/mm) quantification recounts for Observer 1 (ZT, 9 mm).

BLAND-ALTMAN ANALYSIS

Again, difference scores rose with mean IENFD (Figure 3.11) so untransformed plots demonstrated heteroscedasticity (Figure 3.12). The Shapiro-Wilks test for normality of the difference scores returned P-values of 0.075 (Protocol 1) and 0.219 (Protocol 2) for transformed data confirming that calculation of the 95% CI for the RC was appropriate. Differences on averages regression (DA.reg, MethComp) was used to assess the effect of the logarithmic transformation and following the logarithmic transformation the null hypotheses of constant differences between methods (P-value for Protocol 1: 0.835; P-value for Protocol 2: 0.741) and residual variance (P-value for Protocol 1: 0.431; P-value for Protocol 2: 0.273) could not be rejected. Bland-Altman statistics produced from log-transformed data are presented in Table 3.7.

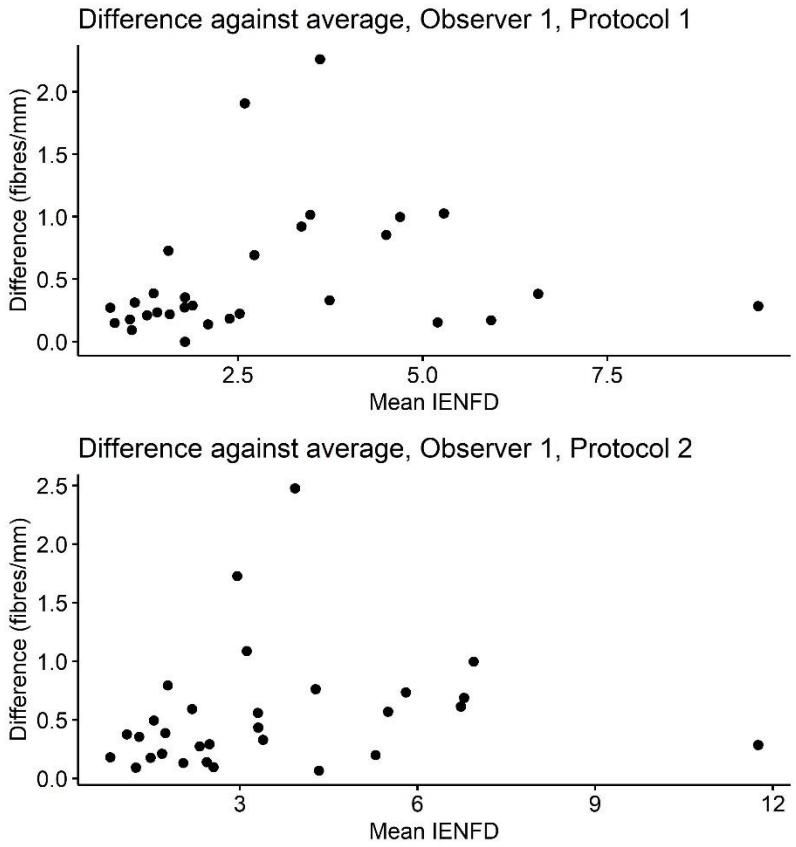

Figure 3.11 Intra-observer differences versus averages plots, Observer 1 (ZT, 9 mm).

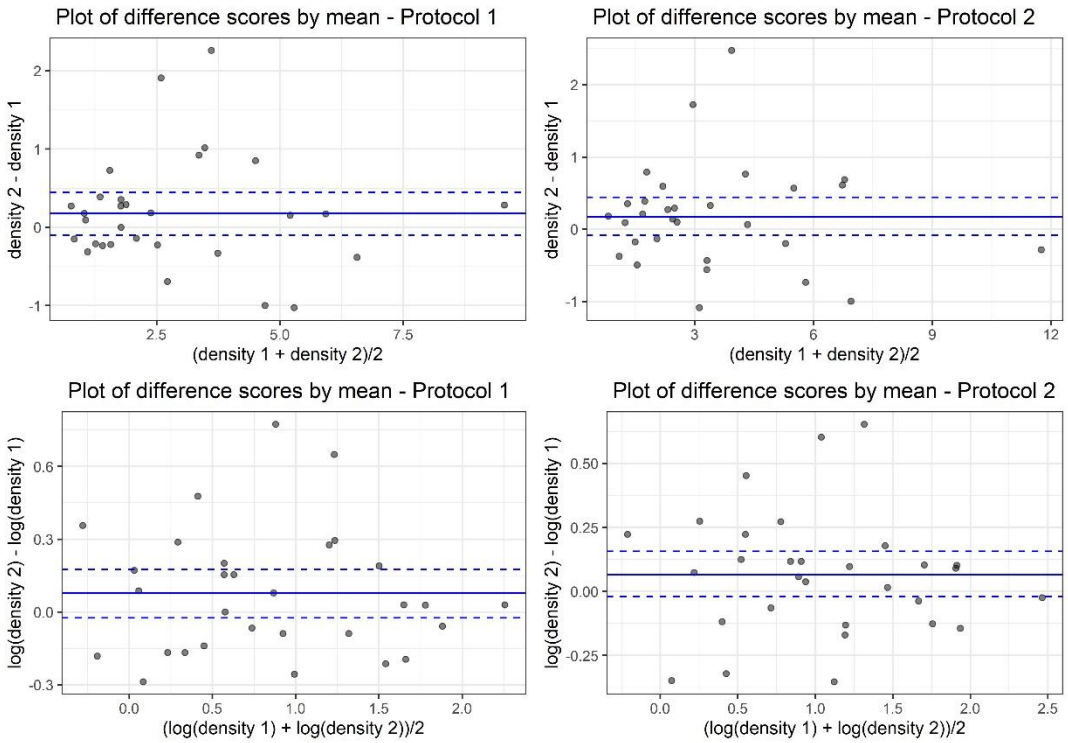

Figure 3.12 Difference scores by means plots for Observer 1 (ZT, 9 mm).
Continuous line – bias of differences. Dashed line – 95% CI of bias of differences.
Upper plots – untransformed data. Lower plots – log transformed data. Density – IENFD.

Statistic	Protocol 1	Protocol 2
Mean Difference	0.18	0.17
Geometric Mean Ratio	1.08	1.07
Log density SD_d	0.260	0.241
Log density RC as ratio (95% CI)	1.667 (1.505 – 1.981)	1.604 (1.459 – 1.882)
Log density RC % (95% CI)	66.7 (50.5 – 98.1)	60.4 (45.9 – 88.2)

Table 3.7 Bland-Altman intra-observer repeatability statistics, Observer 1 (ZT, 9 mm).

Analysis for samples with low mean density was not undertaken, as repeatability was poorer for quantification on ≥9 mm of epidermis compared to ≥20 mm, at a level which may be clinically significant, based on the respective RCs.

Other Repeatability Measures

Typical errors based on log transformed data are presented in Table 3.8.

Statistic	Protocol 1	Protocol 2
Typical percentage error estimate (Log density)	18.4	17.1
Typical error – reduction in measure % (90% CI)	15.5 (12.8 – 19.8)	14.6 (12.0-18.7)
Typical error – increase in measure % (90% CI)	18.4 (15.2 – 23.5)	17.1 (14.1 – 21.9)

Table 3.8 Intra-observer typical error, Observer 1 (ZT, 9 mm).

Interpretation

Typical error for Protocol 2 was 17.1% and the repeatability coefficient was 60.4%. Based again on the minimum IENFD for Protocol 2 obtained by Observer 1 (0.77 fibre/mm), the maximum measured IENFD for which we could be 95% confident repeat quantification would fall below the reference interval would be 0.41 fibres/mm (0.66 ÷ 1.60).

Observer 2

Twelve Zamboni's-fixed samples from the proximal site were quantified using ≥9 mm of epidermis from at least 3 sections. Each tissue section was subjected to IENF counting twice. The mean length quantified was 11.98 mm. In order to provide a direct comparison between observers, this data set was also analysed for Observer 1. Results for both observers are shown in Figure 3.13.

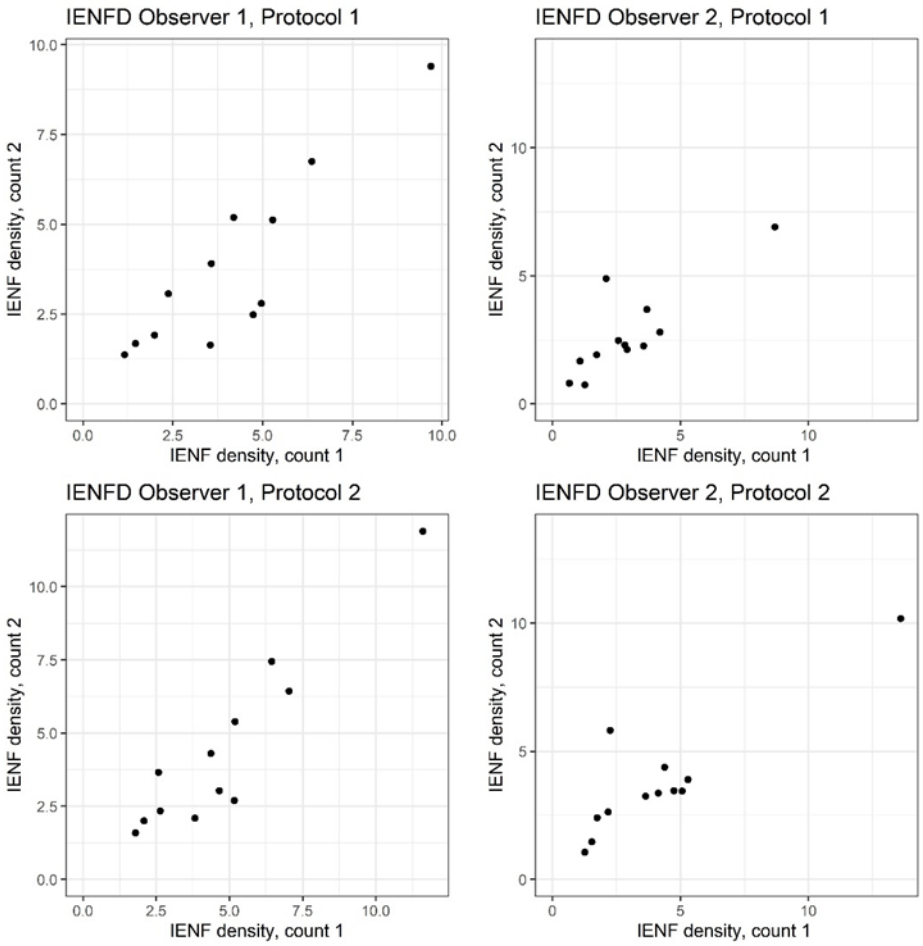

Figure 3.13 Observer 1 and Observer 2 IENFD (fibres/mm) quantification recounts (ZT, 9 mm).

Bland-Altman Analysis

Bland-Altman statistics and descriptive statistics for this data set are presented in Table 3.9. For Observer 2, (as for Observer 1) Protocol 1 had a higher repeatability coefficient (2.20, 95% CI; 1.76 – 3.68 as ratio) compared to Protocol 2 (2.08, 95% CI; 1.69 – 3.37 as ratio). Additionally, Observer 2 had a higher repeatability coefficient for Protocol 2 than Observer 1 (1.79, 95% CI; 1.53-2.61) however, confidence intervals are overlapping. Observer 2 had a lower systemic bias of the differences (geometric mean ratio) for both protocols compared to Observer 1, however for all systemic biases reported, zero (geometric mean ratio = 1) fell within the 95% CI of the bias of the differences (plots not shown).

Statistic	Protocol 1 Observer 2	Protocol 1 Observer 1	Protocol 2 Observer 2	Protocol 2 Observer 1
Geometric mean ratio	1.05	1.10	1.03	1.13
SD_d (log data)	0.40	0.36	0.37	0.30
Repeatability Coefficient as ratio (95% CI)	2.20 (1.76 – 3.68)	2.02 (1.65 – 3.18)	2.08 (1.69 – 3.37)	1.79 (1.52-2.61)
Mean IENFD (fibres/mm)	2.83	3.94	3.97	4.59
Median IENFD (fibres/mm)	2.54	3.67	3.89	3.89
10^{th} percentile (fibres/mm)	1.04	1.61	1.56	2.08
5^{th} percentile (fibres/mm)	0.88	1.43	1.35	1.88

Table 3.9 Statistics for Observer 2 versus Observer 1 (ZT, 9 mm).

INTERPRETATION

There was a trend for a more consistent differences (lower repeatability coefficient) but higher systemic bias of differences for Observer 1 using Protocol 2. There was also a trend for lower IENFD for Observer 2 compared to Observer 1. No significant differences in the repeatability coefficient between observers were demonstrated, however the repeatability coefficient for Observer 2 was 108%, compared to 79% for Observer 1.

3.3.2 Inter-observer reproducibility

For inter-observer reproducibility Bland-Altman, limits of agreement were calculated (as if for method comparison) on a data set comprising 12 subjects where ≥9mm epidermal sections (identical for both observers), had been assessed. Method comparison analysis is considered appropriate for inter-observer analysis, as opposed to repeatability analysis (producing RC), as significant systemic bias of differences is likely. Results for Observer 2 versus Observer 1 are shown in Table 3.10. Differences on averages regression and Shapiro-Wilks tests were used to check assumptions were valid for log-transformation of data and for CI calculation, as before.

Statistic	Protocol 1	Protocol 2
Mean Difference	-1.12	-0.63
Estimated geometric mean ratio	1.433 (1.24 – 1.65)	1.19 (1.01 – 1.41)
Lower limit of agreement ratio	0.92 (0.72 – 1.19)	0.71 (0.53 – 0.95)
Upper limit of agreement ratio	2.21 (1.73 – 2.83)	2.00 (1.49 – 2.71)

Table 3.10 Bland-Altman statistics for inter-observer reproducibility (ZT, 9 mm).

INTERPRETATION

For Protocol 2, for a measured value produced by Observer 2, limits of agreement suggested that the value produced by Observer 1 would be between 29% lower and 100% higher. However, due to the small sample size confidence intervals for the limits of agreement were wide.

3.3.3 Intra-sample reproducibility

First counts for Observer 1 (≥20 mm) were used to investigate intra-sample reproducibility.

ZAMBONI'S FIXATIVE

For 10 dogs, A and B series from biopsies fixed with Zamboni's fixative, all obtained from the same 6 mm biopsy sample and assessed by Observer 1, were available for comparison. Plotting the IENFD for each sample obtained in series A against that for the B series (Figure 3.14) suggested no significant correlation for either protocol.

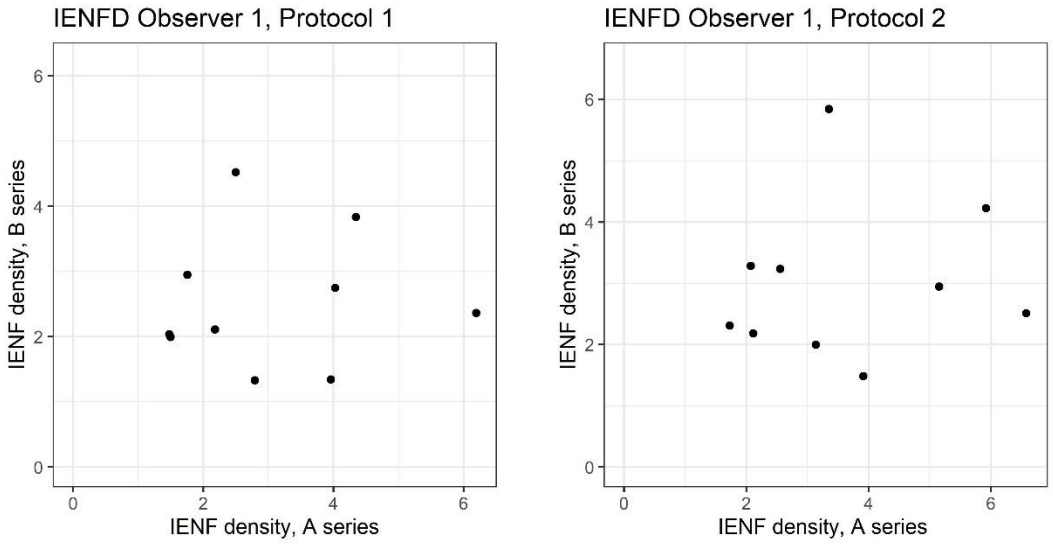

Figure 3.14 Intra-sample IENF quantification results (Observer 1, Zamboni's-fixed, 20 mm).

Whilst sample numbers were small, nevertheless repeatability statistics were calculated to be able to compare intra-sample reproducibility with intra-observer results for recounts of the same sections by the same observer (section 3.3.1).

BLAND-ALTMAN ANALYSIS

For the intra-sample reproducibility, differences on averages regression for untransformed data provided P-values for hypotheses of constant differences and

residual variance of 0.407 and 0.535 for Protocol 1, and 0.276 and 0.797 for untransformed data, respectively. P-values for transformed data were 0.313 (constant differences) and 0.108 (residual variance) for Protocol 1, and 0.295 (constant differences) and 0.200 (residual variance) for Protocol 2. The Shapiro-Wilks test, assessing whether the mean differences were normally distributed, produced P-values of 0.929 for Protocol 1 and 0.945 for Protocol 2 on untransformed data and P-values of 0.392 and 0.360, respectively, for transformed data. Therefore, 95% confidence interval calculations were valid. Differences against averages plots for transformed and untransformed data are shown in Figure 3.15.

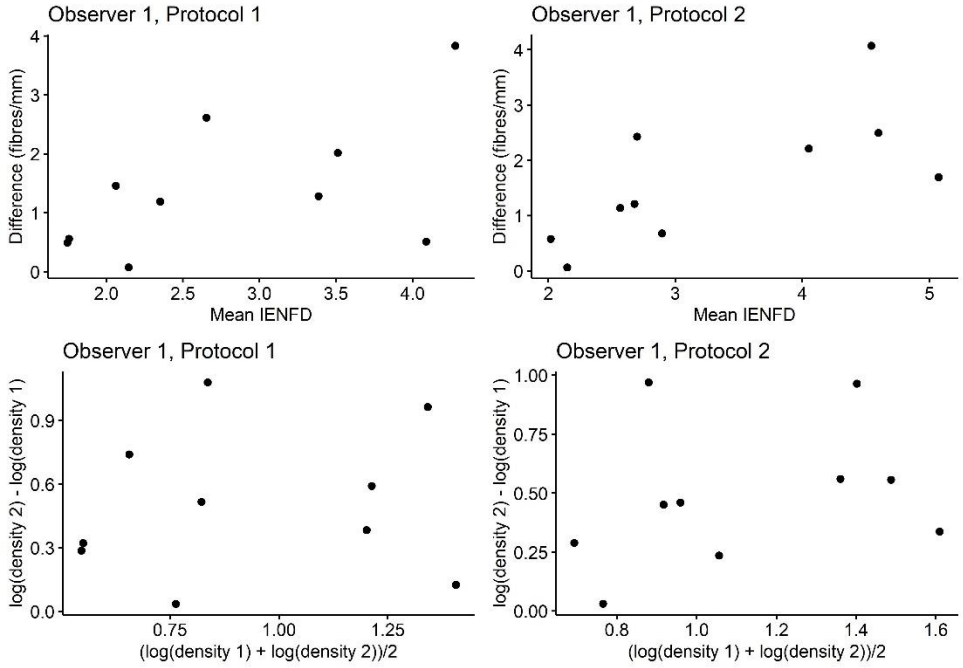

Figure 3.15 Intra-sample differences versus averages plots (Observer 1, ZT, 20 mm).
Upper plots – untransformed data. Lower plots – log transformed data. Density – IENFD.

Bland-Altman statistics for untransformed and log transformed densities and are shown in Table 3.11 and plots in Figure 3.16.

Statistic	Protocol 1	Protocol 2
Mean Difference	0.55	0.65
Standard deviation of differences SD_d	1.78	1.99
Repeatability coefficient (95% CI)	3.49 (2.67 – 5.04)	3.91 (2.99 – 5.65)
Geometric Mean Ratio	1.18	1.19
Log transformed data SD_d	0.610	0.565
Log transformed data RC as ratio (95% CI)	3.308 (2.308-8.174)	3.025 (2.168-6.986)
Log transformed data RC %	230.8 (130.8 – 717.4)	202.5 (116.8 – 598.6)

Table 3.11 Bland-Altman intra-sample repeatability (Observer 1, ZT, 20 mm).

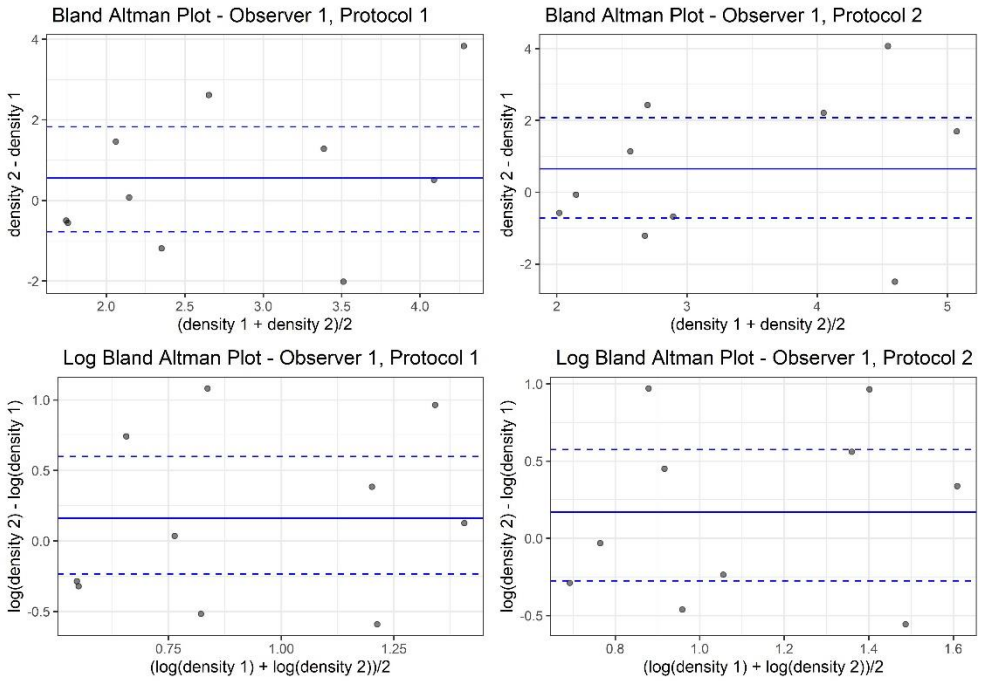

Figure 3.16 Intra-sample difference score by mean plots (Observer 1, ZT, 20 mm).
Continuous line – bias of the differences. Dashed line – 95% CI of bias of differences.
Upper plots – untransformed data. Lower plots – log transformed data. Density – IENFD.

The repeatability coefficient for Protocol 1 was 230.8% (95% CI; 130.8-717.4) and for Protocol 2 was 202.5% (95% CI; 116.8 – 598.6). In contrast to this, the intra-observer repeatability (Observer 1, Protocol 2, section 3.3.1) was 40.1% (95% CI: 31.0 – 57.1) and the lower CI for intra-sample RC was double the value of the upper CI for the intra-observer repeatability RC, indicating that intra-observer repeatability did not represent the source of the lack of intra-sample reproducibility.

Other Repeatability Measures

Typical errors are presented in Table 3.12.

Statistic	Protocol 1	Protocol 2
Typical error	1.26	1.40
Typical percentage error	45.0 (32.8 – 74.0)	42.4 (30.92 – 69.8)
Typical percentage error estimate (Log density)	43.2	39.9
Typical error - reduction in measure % (90% CI)	30.15 (22.0 – 49.6)	28.54 (20.82 - 46.95)
Typical error - increase in measure % (90% CI)	43.2 (31.5 – 71.1)	39.9 (29.1 – 65.6)

Table 3.12 Intra-sample typical error (Observer 1, ZT, 20 mm).

Typical percentage error for Protocol 2 was 42.4% using the untransformed data and the estimate was 39.9% using transformed data. In addition, the ICC for intra-sample repeatability (Observer 1) confirmed no significant correlation between A- and B-

series as the confidence interval included zero: ICC 0.12 (95% CI; -0.51 – 0.67, F(9,9.37): 1.27, P-value: 0.361).

FORMALIN

For 9 dogs, A and B series from biopsies fixed with formalin and examined by Observer 1 were available for comparison. Plotting the IENFD obtained for series A against that for series B (Figure 3.17), revealed little correlation. Further analysis was considered inappropriate due to the small sample size.

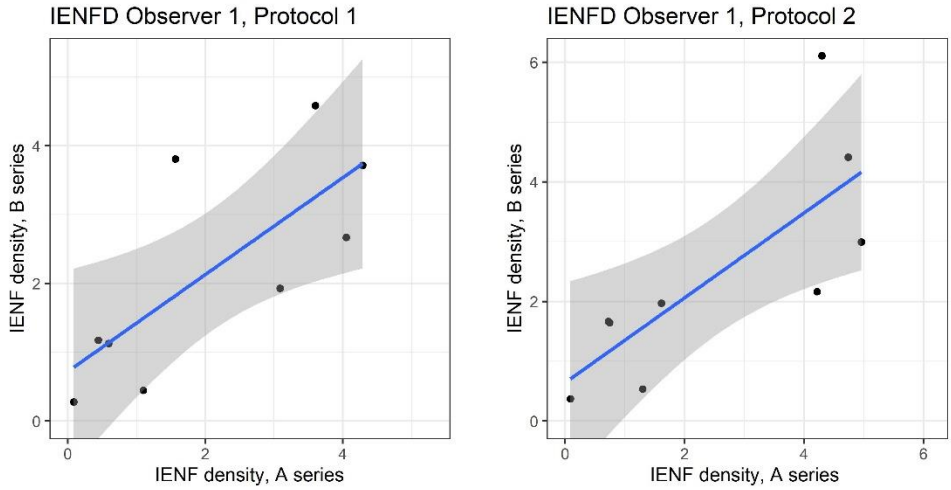

Figure 3.17 Intra-sample correlation of formalin-fixed samples. (Observer 1, 20 mm)
Grey shading: 95% CI for regression line.

COMPARISON OF ZAMBONI'S AND FORMALIN (ALL SECTIONS)

For 7 biopsy sites, both A and B series were available both for Zamboni's fixative and formalin so it was possible to investigate whether there was any correlation in IENFD between formalin fixed versus Zamboni's fixed samples on at least 6 sections (some of which were consecutive sections, i.e. comprised both A and B series), counted by Observer 1. No significant correlation was observed, and further analysis was considered inappropriate (and plots are not shown) due to the small sample size.

Overall, no significant correlation was detected between any of the intra-sample reproducibility data investigated.

3.3.4 Section by section examination

Considering the lack of intra-sample reproducibility on IENFDs derived from multiple sections per sample described above, intra-section reproducibility was examined using ZT samples assessed by Observer 1 (A series).

Intra-observer repeatability for Observer 1, by section, is presented in Figure 3.18, indicating that repeatability of counts for each section is reasonably good, as would be expected, considering the repeatability for Observer 1 for whole biopsy assessment.

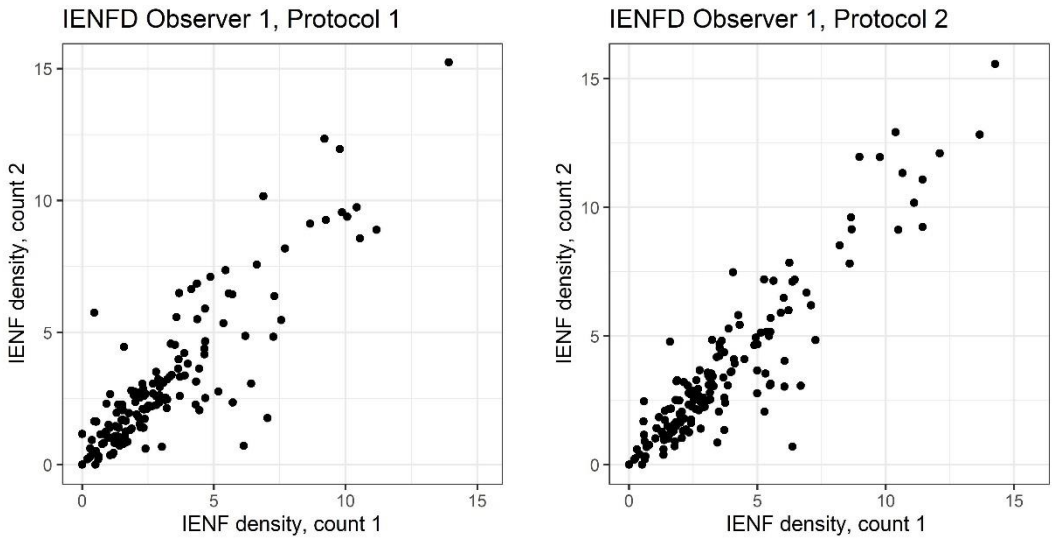

Figure 3.18 IENFD (fibres/mm) quantification recounts (Observer 1, ZT, by section).

Intra-section and inter-section Bland-Altman repeatability analysis were considered inappropriate in this study due to the substantial variation in section length (598 µm to 8539 µm) and in any case was not possible due to rising differences with mean as it was not possible to log-transform data due to IENFD of 0 fibres/mm for some sections. Alternative transformations such as log(x+1) or similar, were not considered appropriate for this analysis. Section variability in IENFD (using the mean of both counts and expressed as individual section read-outs for each sample) is presented in Figure 3.19. demonstrating high within-subject variation in section IENFD in a substantial proportion of subjects under assessment.

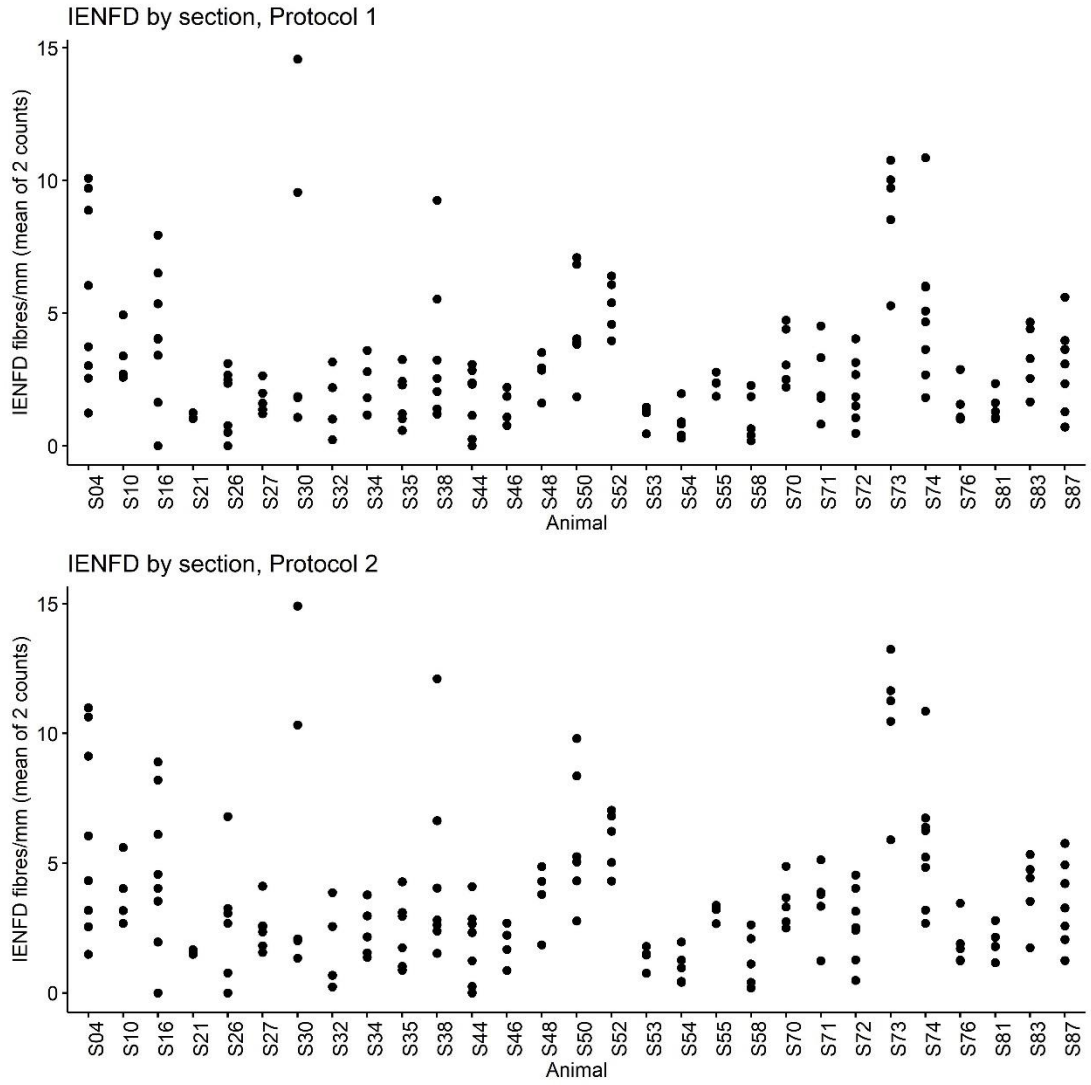

Figure 3.19 Section variability per dog (Observer 1, ZT).
Individual IENFD data points depict values obtained from same sample (including same sampling location, fixation, series and counting protocol) yet different skin sections.

High within-subject variation explains the fact that intra-sample reproducibility is poor compared to intra-observer repeatability. As discussed, section lengths varied widely and therefore the calculated absolute measures of variance must be treated with caution. In order to estimate the average (section by section) within subject coefficient of variation, (within subject standard deviation (SD_w)/mean of true value) the calculation [SD_w/mean density] for each animal (biopsy sample) was used (Barnhart and Barboriak, 2009), and the overall mean taken. As these sections were recounted sections, the mean of the two IENFD recounts was used in order to calculate the SD_w. For Protocol 2 the SD_w was 1.64 and the within subject coefficient of variation was 0.50.

3.3.5 Comparison of Methods

PROTOCOL 1 VERSUS PROTOCOL 2

Limits of agreement for IENFD obtained from Protocol 1 against Protocol 2 (same sections, assessed by Observer 1) were investigated for the ≥20 mm data. For this, Bland-Altman analysis was attempted using both replicates (recounts) (BA.plot, Methcomp package). Differences on averages regression and permutations of replication (DA.reg and perm.repl, MethComp) with replotting were used to assess the effect of the logarithmic transformation. Differences on averages regression indicated that the null hypotheses of the slope of differences versus averages being zero and the variances being constant with mean, could not be rejected for the logarithmic transformation (P-values: 0.018 and 0.182 respectively). However, with increasing mean values for IENFD, there was a trend towards differences becoming more negative (Protocol 2 producing higher values). Therefore, a regression approach for non-uniform differences may have been more appropriate (Bland and Altman, 1999). However, linear regression to assess the bias of differences, fitted by alternating regressions (AltReg, Methcomp), was not successful due to the relatively small sample size and it also was not possible to compare the log-transformed model with a linear regression model. Statistics produced by Bland-Altman methods with log transformation are presented in Table 3.13. The Shapiro-Wilks test assessing the normal distribution of differences produced a P-value <0.001. Therefore, the confidence intervals could not be calculated.

Statistic	Protocol 1 to Protocol 2
Mean Difference	-0.20
Estimated geometric mean ratio	0.82
Lower limit of agreement ratio	0.565
Upper limit of agreement ratio	1.186

Table 3.13 Bland-Altman statistics for comparison of methods, Observer 1 (ZT, 20 mm).

INTERPRETATION

For a given measurement for Protocol 2, Protocol 1 would yield a measurement approximately 44% below to 19% above. However, these results must be treated with a degree of caution as the linear regression approach could not be applied.

4. Discussion and Conclusions

Discussion

The most relevant results with regards to using IENFD to support the diagnosis of peripheral neuropathies in dogs are the poor intra-sample reproducibility (A versus B series and intersection variability within a given biopsy sample) combined with the overall relatively low minimal and median IENFD obtained in this data set (section 3.2). Within the range of IENFD measured in this cohort, there was no significant correlation between intra-sample results, regardless of quantification protocol or fixative under assessment, overall indicating poor reproducibility. Supplementary analysis of an (albeit small) number of biopsy sites allowed further comparison of the IENFDs obtained for two fixatives and using ≥40 mm epidermis from at least 6 sections per fixative. If the reproducibility of IENF quantification using this greatly expanded length of epidermis were good (guidelines for the examination of human skin biopsies recommend the assessment of at least 3 sections from a 3 mm biopsy sample (Lauria et al., 2010a)), then significant correlation between IENFDs obtained from the same sampling region yet exposure to different fixatives might be expected. However, this was not the case. Finally, with counting Protocol 2 (which represents the overall more reliable counting protocol), the typical percentage error for intra-observer reliability on the same sections (12.2%) was considerably lower than the intra-sample error (38.3%), indicating that the lack of correlation / poor reproducibility of the intra-sample data does not stem from poor repeatability by Observer 1, but is the consequence of high inter-section variability within a biopsy sample (section 3.3.4, see also below).

Assessing intra- and inter-observer reliabilities, comparable human studies report a RIV ± SD of 9.6 ± 8.9% for intra-observer reliability and 9.6 ± 9.4% for inter-observer reliability (using IENFD calculated over 2-4 sections) and 10.2 ± 11.9% for individual sections (Smith et al., 2005). Wöpking et al., (2009) report RIV ≥35.6% (no SD given, calculated on individual sections) for inter-observer reliability. In comparison to this, the intra-observer RIV calculated as described by Smith et al. (2005) for Observer 1 (Protocol 2, 20 mm) in the present study was 5.0 ± 17.09%. Smith et al. included intraclass correlation (ICC, see below) for comparisons which in turn included within-subject variation of whole biopsy measures, however did not report RIV for these (Fig1 c and d, Smith et al., 2005). Interpretation and comparison of RIV is further

complicated by the fact that small absolute differences at low IENFD (as seen in this study) produce high percentages. Wöpking et al. (2009) prefer the metrics inter-section SD and relative inter-section SD (interpreted as SD of differences / mean IENFD for individual sections), which is not comparable to whole biopsy metrics reported in the current study. In the present study, for Protocol 2 the SD_w (within subject standard deviation) was 1.64 and the within subject coefficient of variation was 0.50, which lies beyond the maximum readouts reported in the study of Wöpking et al. which reached 0.84 for SD_w (termed inter section SD in that study) and 0.21 for within subject coefficient of variation. This indicates that the within-subject variation in the present study on dogs was higher than that for humans as calculated by Wöpking et al., (2009).

Generally, within-subject measurement variation in human samples, particularly with respect to the actual measurement protocol (i.e. whole sample measures) are only rarely reported. Further support for a potential initial lack of appreciation of the importance of within subject variation (particularly for subjects with borderline - low IENFD) is provided by a more recent study of Engelstad et al., (2012) in which the variation in IENFD in patient sections is used to provide a confidence interval. This study recommends the use of at least 4 sections as standard, rather than the previous recommendation of ≥3 sections (Lauria et al., 2005a). Where confidence intervals straddle the pathological cut-off, then further sections (up to 10) may be counted to reduce the confidence interval (Engelstad et al., 2012).

In general, measured IENFD in this study was low in comparison to IENFD obtained in comparable regions in laboratory animals and humans (Lakritz et al., 2015; Lauria et al., 2005b; Provitera et al., 2016) and in the canine skin sections, the IENF were commonly seen clustering in small groups (as opposed to being distributed evenly throughout the sections). Thus, quantification of a larger number of sections may produce reliable IENFD for any given dog, however based on the results obtained in this study (including the assessment of ≥40 mm of epidermis over 6 sections in some dogs), it is unlikely to be reliably achieved with a single 2-3 mm biopsy sample or the recommendation of assessment of ≥9 mm of epidermis as prescribed for human subjects, and would still be challenging with a 6 mm sample. It may be considered that the use of cadaver samples could have resulted in reduced IENFD in the present study, however for 13 of the 41 dogs for which samples were analysed the PMI was less than

1 hour and PMI made no significant difference to IENFD. Therefore, it is unclear that the use of clinical samples (from normal live dogs) would have resulted in significantly increased measured IENFD.

Also, the results for the intra-observer repeatability (recounts of the same sections), at least for Observer 1, further corroborate the view that based on the results obtained in this study (and bearing the overall low IENFD obtained in this cohort of dogs in mind), the determination of IENFDs would be challenging if not impossible to apply as a diagnostic test in canines. For Protocol 2 the repeatability coefficient was 40.1% and based on the minimum IENFD obtained in this data set (Latimer, 2011) and to be confident that there is a true difference between the normative range in our data set and a patient, the patient would require an IENFD lower than 0.47 fibres/mm. Although sample size was small, the results for Observer 2 suggest an even higher repeatability coefficient (i.e. poorer repeatability of recounts) combined with lower IENFD values compared to Observer 1, overall making a suitable cut-off value even more difficult to achieve. It is unlikely therefore, that this test under the conditions applied in this study could produce suitable cut-off density for normal versus abnormal IENFD, notwithstanding the poor intra-sample reproducibility, considering that the overall relatively low IENFD measured in the haired skin of dogs in this study would require a very high level of reproducibility to identify a suitable cut-off for the identification of abnormally reduced fibre density. In comparison, a normative data set for humans (using brightfield microscopy as in this study) grouped by age and sex, yielded the lowest IENFD cut-off (lower 5^{th} percentile) at 1.8 fibres/mm, which was obtained in males of 70-79 years of age (Collongues et al., 2018). The highest lower 5^{th} percentile lay at 7.2 fibres/mm and was obtained in women of 20-29 years. Examining an example of human patient IENFDs, the mean IENFD (using brightfield microscopy) for patients suffering from progressive sensory neuropathy of the axonal type lay at 2.40 ± 2.30 at the distal leg (Chien et al., 2001). In that study, the 5^{th} percentile cut-off lay at 4.46 fibres/mm, which means that the mean IENFD of affected patients lay at 53% of the cut-off value. If similar conditions were applied to our canine cohort, the mean patient IENFD would lie around 0.33 fibres per mm (6.6 fibres in 20 mm), which is marginally lower than the metric of 0.47 fibres/mm (9.4 fibres in 20 mm) for which we can be confident that repeat quantification on the same sections would not produce a value above the cut-off point. Unless diseased dogs present with

a striking lack of nerve fibres, these very low values obtained leave little scope for IENFD ranges in diseased dogs and creating a suitable balance of sensitivity and specificity.

Normative values for human IENFDs obtained using immunofluorescence are generally higher than those for brightfield microscopy (Lauria et al., 2005b; Nolano et al., 2015; Provitera et al., 2016) and this may provide a suitable alternative. The brightfield method was chosen for this study for two reasons: (a) brightfield microscopy was more readily available (thus facilitating a more rapid turnaround in a diagnostic setting), and (b) visualisation of IENFs for multiple examinations over a prolonged period required consistent staining, in turn thought to be more reliably achievable with brightfield stains. Due to the technical difficulties and therefore, time taken in producing good quality processed samples, and considering the impacts of COVID-19 lockdown, it was not possible to investigate immunofluorescence as an alternative method at the point where generally low IENFD was confirmed in samples.

In humans, advancing age and male sex are associated with a reduction in IENFD. Here, no significant differences were seen; indeed, mean and median IENFD increased with age. However, the effect of age and sex on IENFD in dogs is yet to be examined and large scale normative data for any species other than humans and data for haired skin are scant (Mangus et al., 2016), with most animal studies focussing on the (non-haired) footpad of mice or rats. One such study reports no significant difference in footpad IENFD between normal Sprague-Dawley rats aged 8 weeks and 24 weeks (Lauria et al., 2005b). Any comparison between species is of dubious value however; macaque skin from above the lateral malleolus, for example, can have hundreds of nerve fibres per mm in 50 µm sections (Lakritz et al., 2015). The only previous study successfully investigating IENFD in normal dogs and limited to examining 10 beagles of the same age (15 months; four females and six males), reached a mean IENFD at the calf of 5.92 (95% CI; 4.11-7.74) fibres/mm using 20 µm thick sections (Alves de Medeiros et al., 2009), compared to a median of 3.10 (interquartile range (IR) 1.80 – 3.90) IENFD for 50 µm sections at the proximal site in the present study.

Factors Considered to Potentially Affect IENFD

In the current study, no significant difference in IENFD was found between proximal and distal sites. In humans, IENFD decreases distally (McArthur et al., 1998), which

potentially may reflect a typically larger distance in humans between proximal and distal sampling sites. No difference was found either between IENFD measured using Zamboni's fixed and formalin-fixed tissues, although the number of subjects where IENF quantification was carried out on formalin-fixed samples was small. Studies on human skin indicate that formalin-fixed samples underestimate IENFD by 20% compared to 2% PLP (a standard fixative used in IENF quantification, considered comparable with Zamboni's fixative) and a maximum formalin fixation time of 18 hours is recommended (Kennedy et al., 2005). Whilst this study revealed no significant difference in IENFD due to PMI or fixation time, subjectively, occasional formalin-fixed samples demonstrated marked fragmentation of IENF compared to Zamboni's fixed samples and in general, it appeared that longer PMI (over 18 hours) also contributed to fragmentation, both of which obviously could lead to an underestimation of IENFs. A small number of pilot samples (not included in the analysis) underwent fixation in Zamboni's fixative for more than 7 days and these also appeared to demonstrate increased IENF fragmentation. The EFNS guidelines for diagnostic IENF quantification in humans suggest a fixation time of 24 hours for Zamboni's fixative, (Lauria et al., 2005b). However, canine skin blocks fixed for this interval were not firm enough for cutting using the techniques described here, and a minimum fixation time of 64 hours (3 nights) in Zamboni's fixative, or 40 hours for formalin, were required to reliably produce adequate sections. As the aim of this study was to assess the practicality of these methods for use in a diagnostic setting, samples were not processed over the weekend, resulting in a range of fixations times of ≥64 hours. Whether these prolonged fixation times potentially had a diminishing effect on IENFD in this study setting, can only be surmised.

Data Analysis

A variety of statistical methods have been applied to the reproducibility of IENF quantification in human studies and according to one group of authors the use of suitable methods has been limited (Wöpking et al., 2009). Due to the small numbers of subjects, or lack of consistent and comparable IENF visualisation in previous canine studies (Alves de Medeiros et al., 2009; Laprais et al., 2017), no formal repeatability analysis was carried out. In the present study Bland-Altman analysis was considered most appropriate for data analysis, as it provides the ability to compare the outcome (limits of agreement or repeatability coefficient) to the actual measurements, allowing

for decision making on the suitability of the test based on what likely represent clinically significant differences. In addition, Bland-Altman analysis provides additional detail by also assessing mean difference/bias of differences, therefore, describing both systemic and random variations between measured values. Due to the difference scores rising with increasing mean in many data sets in this study, logarithmic transformation of the data was applied, producing results as ratios (which were converted to percentages).

Correlation will not be discussed in detail as not only a high correlation, but also intraclass correlation can conceal lack of agreement (Atkinson and Nevill, 1998; Bland and Altman, 1986), with the difference between calculation of the Pearson correlation coefficient and ICC being that ICC does not depend on the order of values in each of the data pairs, but estimates the average correlation among all possible permutations of order of data pairs. ICC and correlation are both sensitive to data range (Popović and Thomas, 2017) and do not allow direct comparison with measurements in the way that the LoA or RC do. These latter measures therefore, were considered superior for our purposes, by allowing for comparison to a potentially clinically significant difference. Nevertheless, selected ICCs were calculated in this study in order to allow comparison with other studies. Intra-observer correlation for Observer 1 was 0.96 (95% CI 0.92 – 0.98), comparable to values reported in Smith et. al (0.98). The ICC for intra-sample reproducibility in the present study was 0.12 (95% CI -0.56 – 0.669). In comparison to this, one study on human subjects investigating within subject variation (McArthur et al., 1998) by comparing separate series of slides from both the same punch and separate punch biopsies reached a correlation coefficient of 0.86.

Tissue Processing

Several technical challenges were encountered in tissue processing throughout the project (for specific details of optimisation of the final protocol, see Appendix C), the most relevant aspects of which are discussed below.

Maintaining the integrity of tissue sections during staining was extremely challenging and many sections were discarded due to damage or folding. In many cases, separation occurred between the superficial and deep dermis and in some, the epidermis became detached from the dermis. Care was taken to reduce folding of tissues during processing, but this could not always be avoided. In some sections, it was suspected

that separation or folding of tissues during processing (even folding which may have been unnoticed and later rectified) caused inconsistent staining of nerve fibres throughout the section by reducing or increasing ("edge effect") access of staining reagents to certain areas of tissue sections. To mediate any such effects, quality control at the epidermal measurement stage (using epidermal and dermal nerve fibre staining quality and assessing sections for folded or separated regions) resulted in many sections being rejected. In general, the final staining protocol was aimed towards the bare minimum of tissue handling and minimising the use of any reagents likely to cause tissue damage, which is why for example bleaching, which adds tissue handling steps and the exposure to caustic reagents, was omitted in the final processing protocol. Most sections did not require bleaching and tissues were also not bleached in another study of IENFD in dogs, where it was considered that melanin granules could be differentiated from IENF (Alves de Medeiros et al., 2009).

Although the fragility of human skin also provides a challenge in the protocols of human IENF quantification, there are reasons to suggest why canine skin appears to survive free-floating staining techniques with less success. The epidermis of the haired skin of dogs only contains 2-4 layers of living cells (Affolter and Moore, 1994; Maudlin and Peters-Kennedy, 2016), although the number of cell layers varies between breeds (Theerawatanasirikul et al., 2012). In comparison to this, the epidermis of humans typically has 9-11 layers of living cells (Betts et al., 2013) and contains dermal papillae and rete ridges (Ross et al., 1995), which are absent in canine skin (where numerous hair follicles help anchor epidermis to dermis during life). It was noted that sections from 'thin skinned' breeds such as lurchers were particularly fragile. Additionally, the presence of hair follicles at high density appeared to increase fragility and for one such dog successful processing of biopsies was impossible. Finally, differences in the composition of the dermis (such as the extent of collagen and adipose tissue) between species, breeds and individuals, may also have a bearing on structural integrity.

IENF Quantification

A particular challenge when assessing densely haired skin for IENFD is the proportion of follicular epidermis and some studies on human IENFD specify that only interfollicular epidermis should be used (Collongues et al., 2018). The ease of avoiding

large numbers of hairs in human skin biopsies is perhaps illustrated best by the advice to include ‘a hair’ in the skin biopsy where investigation of hair follicles is required (Lauria and Lombardi, 2012). In macaques, hair follicles are considered to result in variation among sections and to obscure IENF visualisation (Mangus et al., 2016) and, as discussed previously, many animal model studies investigating IENFs use non-haired skin (Hsieh et al., 2000; Jolivalt et al., 2016; Mangus et al., 2019). Some researchers further believe that standardising the orientation of hair follicles in samples is critical for detailed examination of skin innervation (Hendrix et al., 2008). In the current study, careful attention was paid to the orientation of skin samples at embedding. However, upon microscopic examination, the success of this was unclear, possibly due to the pre-clipping of some samples, or because of variations in the orientation of hair within samples. The different samples assessed in this study exhibited variable densities of hair. In many samples it was difficult to completely avoid any follicular epidermis, whilst in some sections, it was impossible to tell if most of the measured epidermis included the upper reaches of follicles, or if undulating surface topography was due to the numerous skin folds seen in many dogs and aptly illustrated in a study on the morphology of canine skin, which suggested the extent of folds is breed-related (Schwarz et al., 1979).

Clarity of the dermo-epidermal junction is considered an important factor in the reproducibility of IENF quantification (Wöpking et al., 2009) and the skin folds in canine skin likely contribute to this junction often being indistinct and shifting position throughout the 50 µm skin sections used in this study. Schwarz et al. (1979) report that at the base of these skin folds the epidermis is thin and layers are indistinct. This fits with our findings that Protocol 1 (which used the first basal layer of cells as a cut-off for counting short fibres), was less reliable than Protocol 2, as the basal layer was not well defined. Examination of 20 µm sections stained with Periodic-acid Schiff to highlight the basement membrane revealed unclear staining in these relatively thick sections of dog skin and it was felt that the ability to focus on individual (predominantly epidermal) nuclei throughout the section would aid in locating the junction. Hence, nuclear staining was used in preference to direct staining of the BM to identify the dermo-epidermal junction in the present study. Despite relative clarity of the dermo-epidermal junction, deciding whether a nerve fibre was crossing the BM as its location shifted, or was entering the plane of the section from within the

epidermis, was often very challenging. Additionally, it relatively often appeared that single fibres left and re-entered the epidermis within a section, a phenomenon not described in protocols for IENF quantification in humans. Finally, one of the conditions specified in the EFNS guidelines for IENF counting may be less applicable to dogs; Kennedy et al. state that nerves which branch after crossing the basement membrane should be counted as one unit because nerve endings in normal subjects, in comparison to patients with neuropathy, are usually simple with minimal branching (Kennedy et al., 2005). In the current study, there was often complex intraepidermal branching, which may be related to the skin folds of the dog. Possibly, fragment counting methods as applied in some animal studies (Christianson et al., 2003; Davidson et al., 2010; Höke et al., 2003) may give more reproducible results than those here reported, or at least would ease the decision making process, speeding up quantification.

Breed-related differences specifically relating to the hair coat and follicles may further complicate the aim of producing normative values for IENFD in dogs thus limiting the clinical application of such a test. It has been shown that at least in mice, interfollicular IENFD is related to the stage of the hair cycle (Botchkarev et al., 1999; Hendrix et al., 2008; Peters et al., 2001). Whilst in dogs the relationship between the interfollicular IENFD and the hair cycle has not been investigated, it may not be entirely unexpected that remodelling of epidermal tissue in any species as observed in mice is associated with remodelling of, or changes to, innervation and therefore perhaps, increased IENFD. Certainly and the other way round, damage to peripheral nerves in dogs can cause regional alterations to hair growth (Paus, 1997). The exact association between hair cycle and innervation is complex, however, neuropeptides and nerve growth factor are involved in regulation of the hair cycle (Peters et al., 2006a, 2006b). Some dog breeds (such as arctic breeds) have more synchronous hair cycles than others and a difference can be observed in the ratio of telogen and kenogen follicles throughout the year (Welle and Wiener, 2016), which in turn may result in IENFD changing with the season. Poodles have up to 98% of follicles in anagen at any one time, whilst most other breeds have up to 34% of follicles in telogen (Welle and Wiener, 2016). Furthermore, mice in telogen exhibit few IENFs and thin epidermis, mice in early anagen exhibit dense epidermal innervation, whilst mice in late anagen exhibit decreasing epidermal innervation and a thicker epidermis (Hendrix

et al., 2008). If the same applies to dogs, hair cycle related changes to the skin thickness could additionally affect IENF quantification, through altering ease of visualisation.

LIMITATIONS AND FUTURE WORK

The lack of agreement between intra-sample sets of sections examined in this data set suggests that achieving reproducibility of IENF quantification in the haired skin of dogs is difficult, if not impossible, although examining a larger number of more widely spaced sections and a larger number of subject samples may be useful. Considering those results, it was not possible to produce a reliable cut-off value to help identify reduced IENFD or to comment on the true effect of sex, age or other variables on IENFD in the dog. As discussed, stage of the hair cycle, season and breed may also have effects on IENFD in the dog and a large study demonstrating good reproducibility would be required to evaluate a suitable cut-off value or group cut-off values for dogs. Investigation of protocols which include fragment counting to take into account complex epidermal branching, as commonly seen in dogs and not specifically described in relevant counting protocols in humans, and alternative methods for increasing dermo-epidermal junction clarity may be warranted. Immunofluorescence techniques were not investigated in this study and these, combined with further refinement of fixatives and potentially decreased fixation periods, may be useful in increasing the quantified IENFD, thereby aiding the production of a higher cut-off value and mitigating the need for very high reproducibility. Also, as previously discussed it is unclear whether the use of cadaver samples may have resulted in reduced IENFD measured in this study. Intra-observer reproducibility only using Zamboni's fixed sections (and not formalin-fixed sections) was investigated. Another limitation of the methods described here, was the inability to process samples from some dogs due to extreme tissue fragility. Further investigation of the suitability of canine footpads including bleaching protocols and determination of clinical viability may provide a suitable alternative, as this tissue appears to suffer from less handling artefact and avoids hair cycle effects. No clinical samples were obtained during this study and dermal fibres were not analysed. However, dermal nerve fibres could be visualised using the methods in this study. In people, dermal nerve quantification can be used in conjunction with IENF quantification to increase the diagnostic yield of skin biopsy in small fibre neuropathies (Merkies et al., 2015; Vlčková-Moravcová et

al., 2008) and aid in determining an aetiological diagnosis. For example, subepidermal nerve plexuses are involved in diabetes mellitus, toxicity and autoimmune disorders but are described to be within normal limits in small fibre neuropathies of other aetiologies (Sommer, 2019). In such studies, the area or volume occupied by dermal nerve fibre bundles was measured, which lay beyond the scope of the current study.

Conclusions

This thesis has provided evidence that processing of the haired skin for examination of IENFD is possible for most dogs but technically is very challenging. Reproducibility of IENF quantification was poor using ≥20 mm of epidermis (derived from at least 3 sections) due to high apparent within-subject variation when examining two different section sets obtained from the same sample. If the IENFD values obtained in this study cohort represents a true representation of the population, then using these values to produce reliable diagnostic cut-off value for IENFD in the dog is unlikely to produce a useful test, even if reproducibility could be improved. Due to the intra-sample variability, no conclusions on the effect of factors such as age, sex, breed or fixative on IENFD could be made.

To further investigate skin biopsy as a useful test for peripheral nerve disease in dogs, investigation of IENF quantification on footpads, or possibly in larger numbers of sections of haired skin, including immunofluorescence techniques, use of samples from live animals rather than cadaver samples, potential changes to fixation protocols, and consideration of effects of the hair cycle and breed as well as age and sex would be recommended.

5. APPENDICES

Appendix A Sampling Forms

OWNER CONSENT AND INFORMATION FORM:

Investigating the use of skin biopsies to replace nerve biopsies in the diagnosis of certain nerve diseases in dogs and cats

OWNER INFORMATION SHEET and CONSENT FORM

Background: The examination of peripheral nerves under the microscope is occasionally required to support the diagnosis and help choose treatment in some nerve disease in cats and dogs. Recent investigations in humans have indicated that, for certain nerve diseases, the examination of nerves within a skin biopsy can replace the examination of a nerve sample. The sampling of skin in comparison to nerve is safer, easier, cheaper and overall is associated with a much lower risk.

Aim: To examine the potential of using skin samples instead of nerve samples to support the diagnosis of certain nerve diseases, including small fibre neuropathies and immune-mediated peripheral nerve diseases. Findings will be publicised (in an anonymous fashion) at scientific meetings and in the scientific literature.

Requirements: Four skin samples from the hindlimbs, each with a diameter of 5-10 mm. These samples will be obtained after the death of the animal (as soon as possible after death). Additionally, we require details of your pet's age, breed and gender, and a brief description of any recent or ongoing health issues.

Animal's Name	
Age	
Breed	
Male / Female	
Neutered (Yes / No)	

Does the animal have diabetes mellitus? Y/N:

Does the animal have a peripheral neuropathy? Y/N:

If yes, then what neuropathy has been diagnosed (if known)?

Has the animal recently received chemotherapy? Y/N

Is the animal hypothyroid? Y/N

Please briefly describe any other recent or ongoing major health issues:

(Any tissue not used in this first instance will be saved and may be re-used in future associated studies. Associated data will be stored securely for 10 years, after which it will be destroyed.)

This project has been approved by University of Glasgow School of Veterinary Medicine Ethics Committee (13a/17).

For **further information** please do not hesitate to contact *Angie Rupp* DVM, Dr. med. vet., PhD, FRCPath, Dipl ECVP, MRCVS; University Clinician in Veterinary Pathology; AngelikaFrances.Rupp@glasgow.ac.uk.

I have read and understood the owner information sheet provided for this study and consent for my dog/cat to be enrolled. I understand that I can withdraw my dog/cat from the study at any time.

Owner name/Owner's representative (capital letters): _____

If owner's representative, please state relationship: _____

Signature: _____ Date: _____

Sample ID: Sampling Interval (hours): Name of Vet:

SAMPLING PROTOCOL FOR SUBMITTING VETERINARIANS:

Taking Skin Samples for Nerve Fibre Density Project (Dogs and Cats)

Materials provided:	**Other materials you will need:**
Consent form	Gloves
2 x bijou containing Zamboni's solution (labelled ZT and ZB)	Scissors
2 x bijou containing 10% Formalin (labelled FT and FB)	Forceps
3-6 mm biopsy punch (**can be re-used if still sharp**)	
Cardboard for fixing	

Sampling procedure:

- Ensure that the ***consent form*** is filled in correctly and signed.
- Check that the bijoux in the pack all have the same ***sample identifier*** on them (e.g. S1) and write this identifier on the accompanying documentation or consent form for the animal.
- Insert the ***biopsy punch*** perpendicular to the skin and rotate 45 degrees 3-4 times and remove. Grasp the sample ***gently*** with forceps and cut the connection to the subcutis, if present, with scissors. Place the sample (epidermis up) on a small piece of cardboard and gently press onto the cardboard. Put the sample into the correct bijou of fixative, ensuring the sample is covered.
- Put bijoux back in plastic bag and **place in the fridge** with the consent form.
- **Email** g.chapman.1@research.gla.ac.uk **and include the sample location (which fridge).**

Sample sites (PTO for images):

Please take all 4 samples from the same hindleg, avoiding areas of skin abnormality.

- With the animal in lateral recumbency take ***two samples from the area just caudal the stifle joint*** (Images **T**) – common peroneal nerve biopsy site. (You may be able to palpate the nerve on the lateral aspect of the distal femur / just caudal to the proximal tibia – please take the skin sample at the level of the tibia in this region). Place ***one of these samples (on card) in the bijou labelled FT and the other (on card) in bijou ZT.***
- Take two samples from the distal lateral aspect of the tibia - 1/3 of the way up the leg from the lateral malleolus (**B**). Place ***one of these samples (on card) in the bijou labelled FB and the other (on card) in bijou ZB.***

If you are unsure of the quality of your sample, you can put a maximum of 2 samples from the same site in each bijou (more samples may result in poor fixation).

IMPORTANT INFORMATION

Wear gloves at all times when handling fixatives and keep bijou bottles firmly screwed shut at all times. Any spillage should be immediately wiped up with damp paper towel, and disposed of in clinical waste. Hazard information for Zamboni's solution is as for 10% neutral buffered formalin.

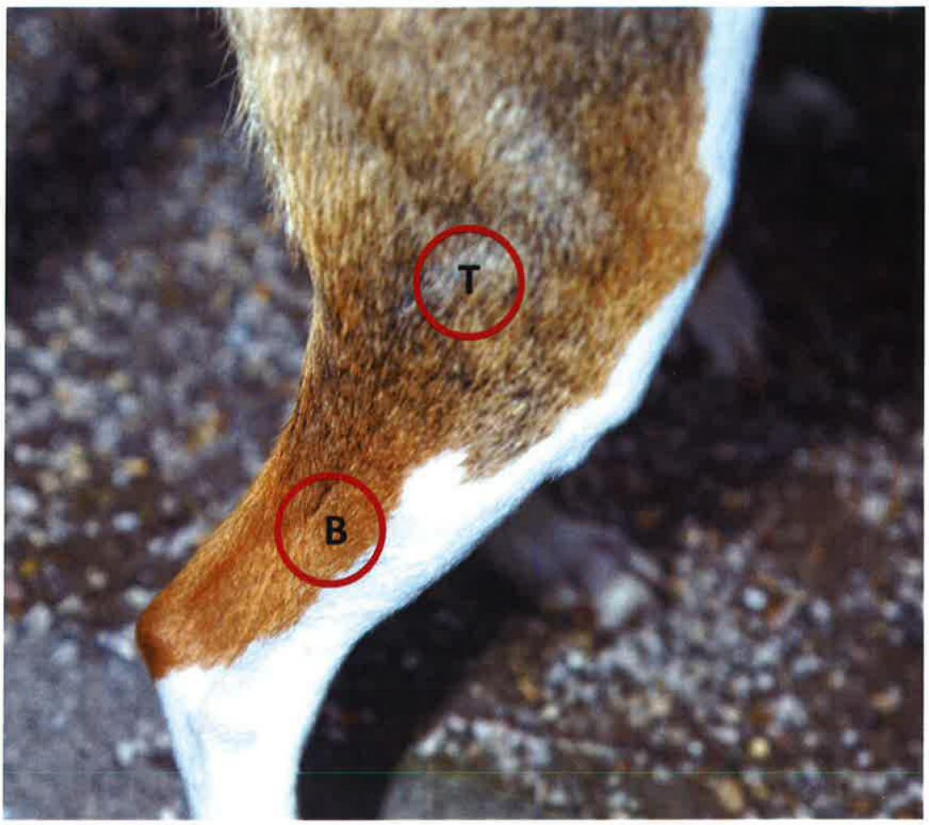

Two samples at site T – One in bottle ZT and one in bottle FT

Two samples at site B – One in bottle ZB and one in bottle FB

Samples need to be picked up within 24 hours (or on Monday morning if taken over weekend).

Vets:
If you would like to be named as an author on any publications (we will include as many contributors as possible – others will be acknowledged) please include an e-mail address with your first sample, and your name on subsequent samples.

Don't forget to put samples in the fridge and get in touch to let us know they are there!

Appendix B Additional Sample Information

Sample	Body Condition Score (/5)	PM interval (h)	Zamboni's fixation time (h)	Formalin fixation time (h)
4	NA	0.5	64	64
10	NA	0	64	64
16	3	2	16	16
21	2	4	16	16
24	3	16	60	60
25	3	4	64	64
26	3	18	112	112
27	2	18	64	64
28	NA	20	64	64
29	2	4	88	88
30	3	4	64	64
31	3	4	136	40
32	3	5	88	40
33	2	18	88	88
34	1	18	64	64
35	2	24	64	64
38	2	4	64	64
40	2	4	64	64
43	NA	0	64	64
44	NA	0	88	88
46	NA	0.5	64	64
48	NA	0	64	64
50	NA	0	88	88
52	NA	0	64	64
53	NA	0	64	64
54	NA	0	88	88
55	NA	0	88	88
57	NA	0	136	136
58	NA	0	64	64
65	2	4	112	112
66	3	1	64	64
67	3	20	64	64
69	2	22	64	64
70	4	4	88	88
71	3	20	88	88
72	NA	23	88	88
73	2	20	112	112
74	NA	2	88	88
75	4	20	88	88
76	3	13	88	88
80	3	26	88	88
81	2.5	12	64	64
82	4	12	64	64
83	2.5	24	64	64
87	5	0	64	64

Appendix C Protocol Optimisation

BIOPSY ACQUISITION

Since tissue sections were fragile, early in the sampling process 6 mm biopsy samples were preferred over 3 mm samples to reduce the number of sections requiring processing.

SECTIONING

The cutting of Zamboni-fixed samples into 50 micron thick sections after a 24-hour period of fixation (as recommended in guidelines for human skin biopsy) was fraught with difficulty, as tissue was not firm enough to produce consistent sections. Therefore, spare tissues (24 tissue blocks, 3 per treatment) were used to investigate ease of tissue sectioning after 18, 40, 64 and 88 hours of fixation with Zamboni's fixative or 10% NBF. A fixation time of 64 hours and 40 hours provided adequate firmness of tissue for cutting tissues following immersion in Zamboni's fixative and 10% NBF, respectively. In conjunction with fixation time, cutting temperatures between -19 °C and -25 °C also were trialled, resulting in an optimum apparent cutting temperature of -22 °C for most tissue blocks. Cutting angles between 0° and 6° were also trialled, with 0° favoured.

Several published (and obtained) hospital protocols use multi-well plates for IHC staining. Therefore, also in this study, transfer of tissue sections into cryoprotectant in 48 well plates was attempted using various techniques (paintbrush, plastic tools, micro loop), yet proved very difficult. Many tissue sections were lost and thaw mounting onto slides and staining of sections directly on the slides was favoured instead.

In order to investigate whether tissue sections could be adequately stained whilst adhered to a slide (as recommended in some available protocols), 12 sections were processed mounted on 3 different adherent slide types (positively charged slides, poly-L-lysine and gelatin coated slides). None of the slide types consistently maintained adherence of tissues throughout the IHC process and therefore, plain glass slides (free-floating technique) were chosen.

BLEACHING

Two bleaching protocols were investigated. Protocol 1 is part of a sample processing protocol used for quantification of IENFD in people, whilst Protocol 2 was adapted from the standard protocol used for bleaching animal skin samples in Veterinary Diagnostic Services, University of Glasgow. For the latter, adaptation was required as this protocol required an incubation temperature of 65 °C for 30 minutes, which was not considered practical for use on free-floating sections in a moisture chamber.

PROTOCOL 1

Room temperature

1. Bleach in 0.25% potassium permanganate for 30 minutes.
2. Remove potassium permanganate and apply 5% oxalic acid for 30 minutes or until colour is removed – several changes may be required.

PROTOCOL 2

1. Bleach in 10% hydrogen peroxide at 37 °C until colour is removed.

In trials, most samples could be subjected to up to 3 hours of bleaching. Longer bleaching times resulted in very fragile tissues which could not be successfully processed for immunohistochemistry.

Overall, neither bleaching protocol was reliably successful in reducing colouration in dog skin to an ideal level in all cases, and for some animals with thin skin and abundant melanin, acceptable tissue condition could not be achieved. However, Protocol 2 was generally more successful for melanin colour reduction.

IMMUNOHISTOCHEMISTRY

Optimisation of primary antibody (PGP 9.5, see section 2.6 Immunohistochemistry) dilution, permeabilization protocols and chromogen application were undertaken.

Primary antibody dilution was optimised using the following protocol:

Following slide preparation, PBS was removed and 3% hydrogen peroxide in methanol was applied and sections were incubated for 45 minutes. Two TBST washes of 5 minutes were applied and after PBST removal, sections were incubated in 1%

normal horse serum (NHS) in PBS for 30 minutes. Excess serum was removed by pipette and a dilution of anti-PGP 9.5 antibody with 2% NHS in TBST was applied and incubated overnight. Two TBST washes of 5 minutes were applied and anti-mouse/rabbit secondary antibody (Vectastain Elite ABC universal kit, Vector Laboratories, Burlingame, California, USA), prepared as per manufacturer's instructions, was applied and incubated for 1 hour. Tissue sections were then washed with TBST twice for 5 minutes. Vectastain enzyme reagents (Vectastain Elite ABC universal kit, Vector Laboratories), prepared as per manufacturer's instructions, were applied and incubated for 1 hour. Distilled water was then used to wash sections twice for 5 minutes. Vector VIP chromogen (prepared as per manufacturer) was applied for 12 minutes before removal.

Antibody dilution IHC run 1:

Each dilution was applied on 1 slide (3 tissue sections per dilution): 1:20, 1:100, 1:500, 1:12500, 1:62500 primary antibody. 1:12500 showed reasonable results (appreciable, consistent axon staining) yet with high background.

Antibody dilution IHC run 2:

Each dilution was used on 3 slides (9 tissue sections per dilution): 1:10000, 1:20000, 1:30000 primary antibody. 1:10000 provided optimal axonal staining with acceptable background when counterstaining was applied.

As Vector VIP cannot be used with aqueous mounting media, primary antibody dilution was further optimised for visualisation each by Vector SG chromogen and 3,3′-Diaminobenzidine (DAB) using dilutions of 1:5,000 1:10,000 and 1:20,000 (6 tissue sections per dilution). For both chromogens again a primary antibody dilution of 1:10,000 was optimal, however Vector SG was considered superior to DAB in differentiating melanin from IENF.

Overall, preservation of tissue integrity during processing represented a priority and therefore permeabilization methods were investigated in order to reduce the use of the tissue damaging agents Tween and methanol. 3 slides (i.e. 9 sections) were processed with each of the conditions described in Table 5.1. For each condition the same 3 tissue blocks from 3 individual dogs, each with thin (i.e. more fragile) skin were used.

Condition	Methanol included in hydrogen peroxide peroxidase blocking step	Tween use
1	Yes	TBST in all washes and primary antibody incubation
2	Yes	TBST in primary antibody incubation only
3	No	TBST in all washes and primary antibody incubation

Table 5.1 Permeabilization conditions tested for IHC.

Nerve fibre staining was apparently identical (clear, consistent) for conditions 1 and 2 and there was little to no staining using condition 3. It, therefore, was concluded that the majority of permeabilization was achieved in the methanol containing step. 9 slides (27 sections) were then processed each for remaining condition (1 and 2) in order to assess any subtle effects on staining and whether reduction in Tween use would benefit tissue integrity. Condition 2 was considered most satisfactory.

Background staining was inconsistent and therefore the incubation times for peroxidase (30 minutes / 1 hour), washes between enzyme and chromogen substrate application (3 x 10 minutes, 3 x 5 minutes and 10 minutes followed by twice for 5 minutes), and chromogen incubation time (10, 12 and 15 minutes) were optimised after counter staining optimisation (see final protocol, section 2.6 Immunohistochemistry).

COUNTER STAINING AND MOUNTING

Due to the fragility of tissue sections it was imperative to keep the number of incubation steps and washes to a minimum and this precluded the use of non-aqueous mounting media due to the extra steps required to dehydrate sections before mounting. Therefore, counter stains which were not suitable for use with aqueous media were not appropriate, which included Periodic-acid Schiff stain, originally considered for staining of the epidermal basement membrane. Alternatively, quantification of IENFD without counter-stain was considered, as this technique, which uses the colour difference between Zamboni's fixed epidermis and the background originating from Vector SG chromogen, is described in the literature. However, this approach was not considered adequate to reliably differentiate the dermal-epidermal boundary in this study due to the frequent changes in its position throughout many of the 50 µm sections of dog skin.

Finally, the utility of nuclear staining with haematoxylin (standard Mayer's haematoxylin and Haematoxylin QS (Vector Laboratories, Burlingame, California, USA)) and nuclear fast red were investigated, whereby the haematoxylin stains produced the better defined staining. However, the intensity of staining with the standard Mayer's haematoxylin was difficult to predict and additional steps were required for decolorizing with Scott's tap water substitute, whereas Haematoxylin QS does not require the use of Scott's. Additionally, the short staining times of a few seconds recommended for standard Mayer's haematoxylin staining were not practical for staining up to 66 free-floating sections, whilst the 5 second minimum staining time recommended by the manufacturer also could not be consistently achieved. The use of Haematoxylin QS was therefore investigated at several dilutions (1:30, 1:40, 1:50) with staining times of 2-5 minutes. A dilution of 1:30 and a staining time of 4 minutes produced acceptable staining intensity on most tissue samples.

Epidermal Measurements

Contrary to studies on human skin, measuring the width of tissue sections did not give an appropriate approximation of length available for evaluation, due to the numerous skin folds and hair follicles encountered in the dog and further exacerbated by significant proportions of epidermis commonly being damaged or folded, in turn the consequence of the greater (perceived) fragility of canine skin when compared to human skin. Therefore, the total length of non-follicular epidermis available for examination was measured.

Pilot Footpad Processing

Footpad biopsies of 3 dogs were investigated for their feasibility to process these samples and whether in these samples the basement membrane/dermal-epidermal junction was easier to appreciate due to a lack of skin folds. For each of these 3 dogs 6 tissue sections were processed. Cutting and maintenance of tissue integrity was superior to haired skin and in one dog basement membrane position was more regular throughout the sections. Of 18 sections only 1 was discarded due to mishap and only 1 was folded resulting in only a short length of epidermis available for examination. However, there was a large amount of melanin in all sections which could not

adequately be reduced by bleaching, and in two animals the basement membrane did not seem significantly easier to clearly identify when compared to that in haired skin.

Appendix D Staining Images

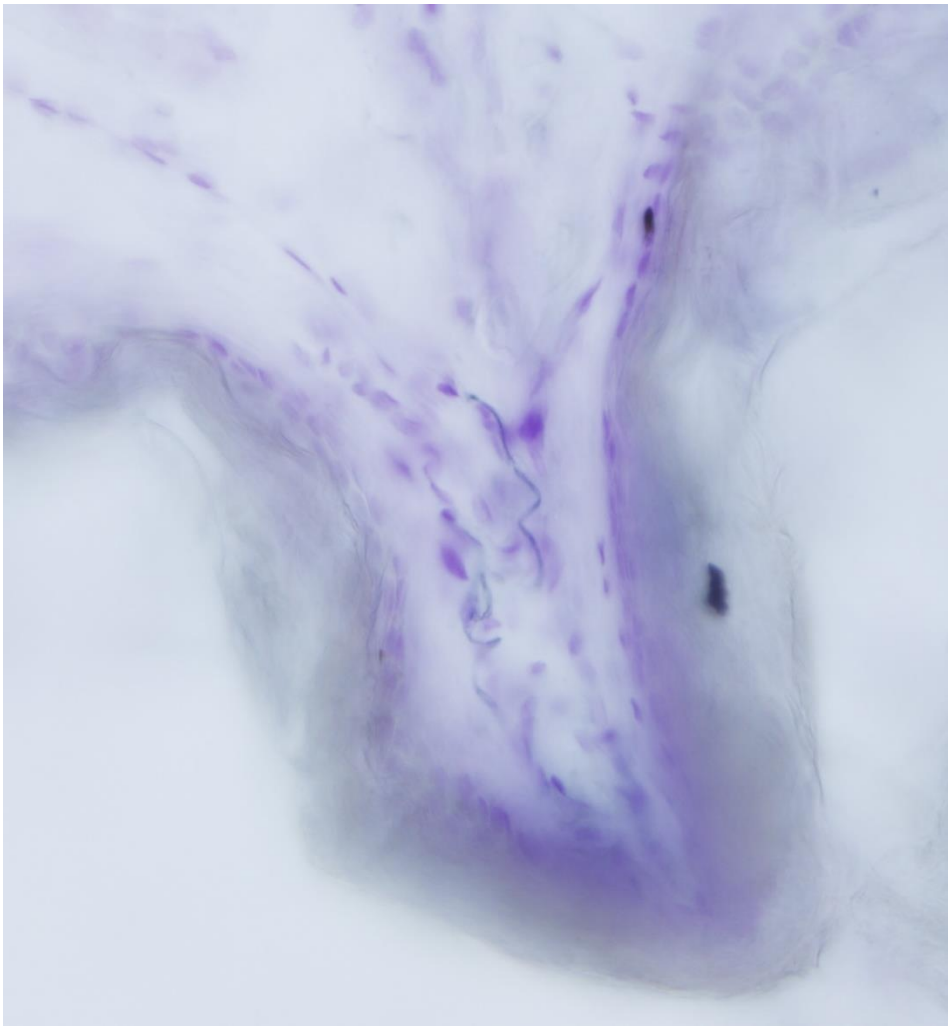

Figure 5.1 Dermal fibre staining.
Nerve fibres stained dark grey-black. Haematoxylin counter stain (x200).

Figure 5.2 Intraepidermal nerve fibre crossing basement membrane.
Nerve fibres stained dark grey-black. Haematoxylin counter stain (x400).

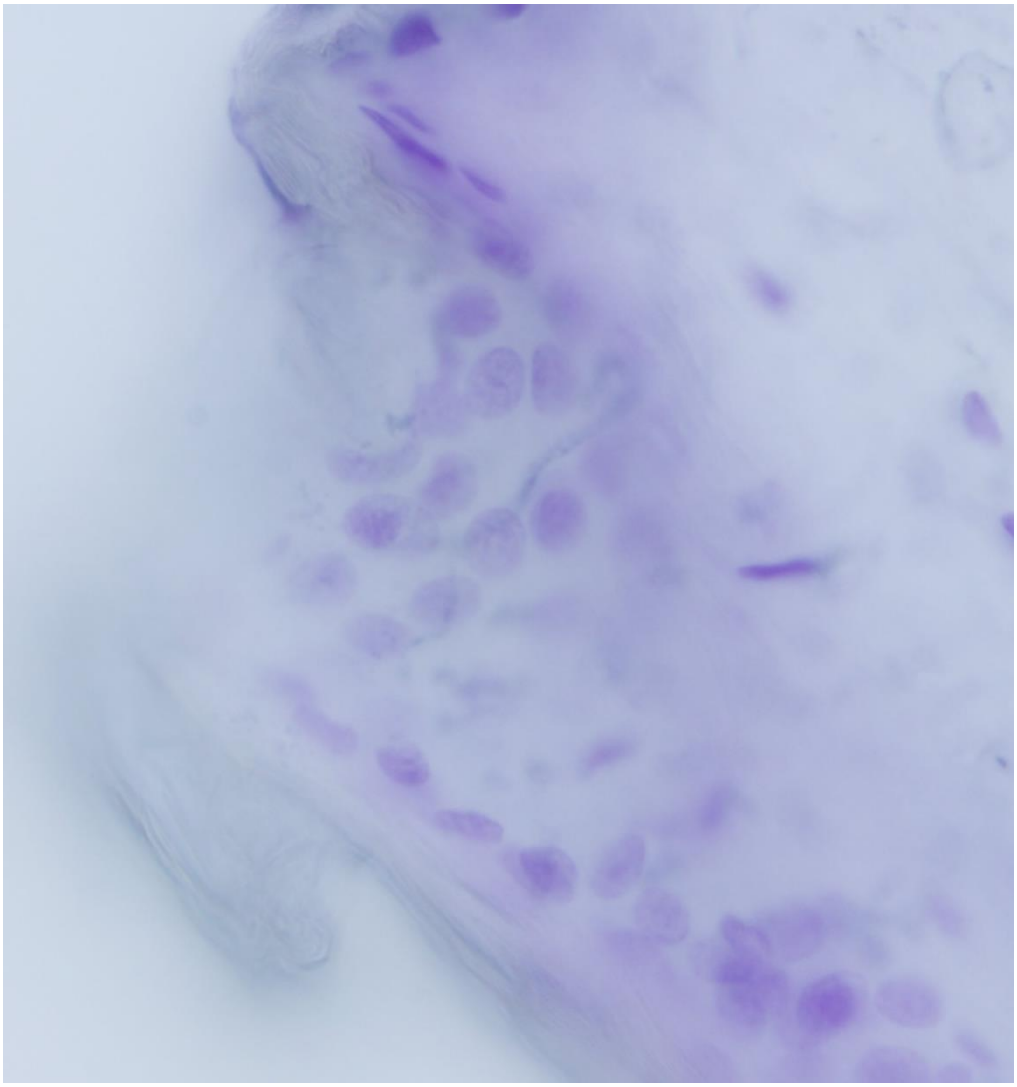

Figure 5.3 Intraepidermal nerve fibre within the epidermis.
Nerve fibres stained dark grey-black. Haematoxylin counter stain (x400).

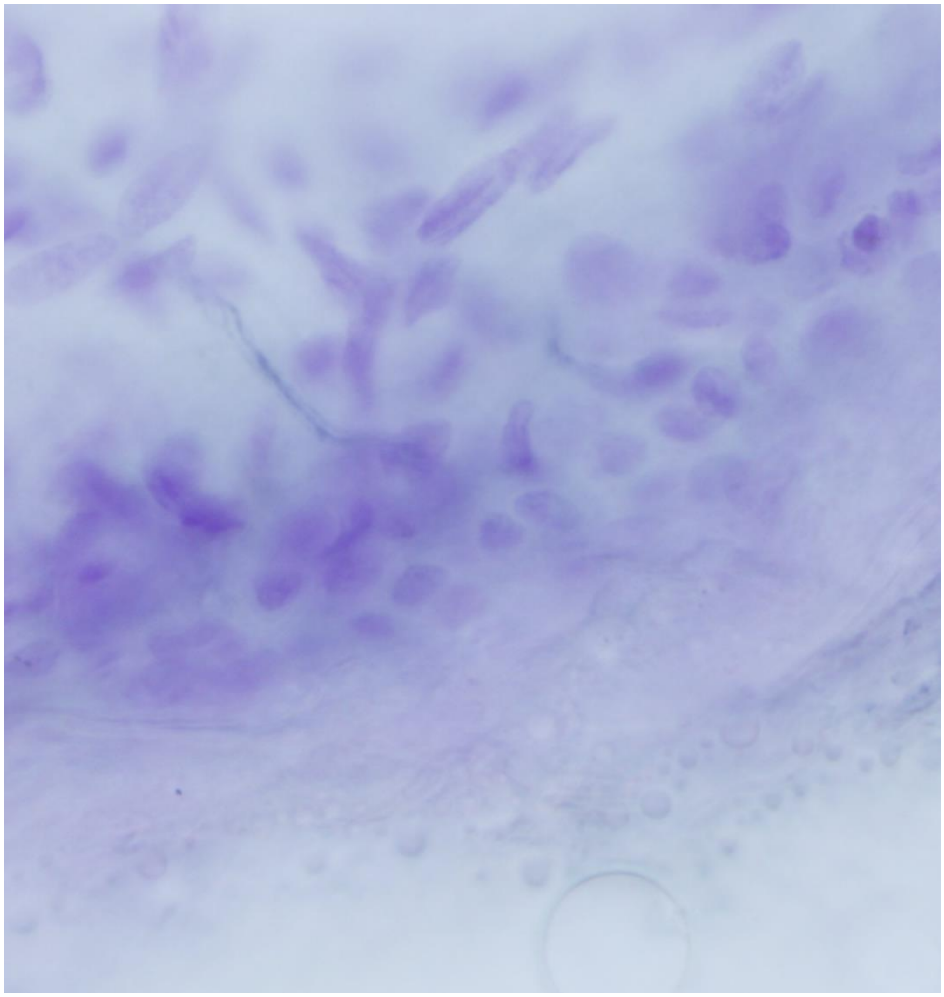

Figure 5.4 Two nerve fibres approaching the basement membrane.
Nerve fibres stained dark grey-black. Haematoxylin counter stain (x400).

Producing images of IENF was incredibly challenging due to the thickness of sections (50 µm). Visualisation and counting required focussing throughout the section in order to follow the course of nerve fibres.

REFERENCES

Affolter, V.K., Moore, P.F., 1994. Histologic Features of Normal Canine and Feline Skin. Clin. Dermatol. 12, 491–497.

Alves de Medeiros, M., Startin, C.M., Jeffery, N.D., 2009. Innervation of canine skin: an immunohistochemical study. Vet. Rec. 165, 314–318. https://doi.org/10.1136/vr.165.11.314

Atkinson, G., Nevill, A.M., 1998. Statistical methods for assessing measurement error (reliability) in variables relevant to sports medicine. Sports Med. Auckl. NZ 26, 217–238. https://doi.org/10.2165/00007256-199826040-00002

Bakkers, M., Merkies, I.S.J., Lauria, G., Devigili, G., Penza, P., Lombardi, R., Hermans, M.C.E., van Nes, S.I., De Baets, M., Faber, C.G., 2009. Intraepidermal nerve fiber density and its application in sarcoidosis. Neurology 73, 1142–1148. https://doi.org/10.1212/WNL.0b013e3181bacf05

Barnhart, H.X., Barboriak, D.P., 2009. Applications of the Repeatability of Quantitative Imaging Biomarkers: A Review of Statistical Analysis of Repeat Data Sets. Transl. Oncol. 2, 231–235.

Betts, J.G., Desaix, P., Johnson, E., Korol, O., Kruse, D., Wise, J.A., Womble, M., Young, K.A., 2013. 5.1 Layers of the Skin, in: Anatomy and Physiology. OpenStax, Houston.

Bio-Rad, 2019. IHC Protocol: Fixative Recipes [WWW Document]. Bio-Rad. URL https://www.bio-rad-antibodies.com/fixative-recipes.html (accessed 5.8.19).

Bland, J.M., Altman, D.G., 1999. Measuring agreement in method comparison studies. Stat. Methods Med. Res. 8, 135–160. https://doi.org/10.1177/096228029900800204

Bland, J.M., Altman, D.G., 1986. Statistical methods for assessing agreement between two methods of clinical measurement. Lancet 327, 307–310.

Botchkarev, V.A., Peters, E.M.J., Botchkareva, N.V., Maurer, M., Paus, R., 1999. Hair Cycle-Dependent Changes in Adrenergic Skin Innervation, and Hair Growth Modulation by Adrenergic Drugs. J. Invest. Dermatol. 113, 878–887. https://doi.org/10.1046/j.1523-1747.1999.00791.x

Braund, K.G. (Ed.), 2003. Neuropathic Disorders, in: Clinical Neurology in Small Animals. International Veterinary Information Service, Ithaca, p. 53.

Carstensen, B., Gurrin, L., Ekstrom, C.T., Figurski, M., 2020. MethComp - Analysis of Agreement in Method Comparison Studies [WWW Document]. URL https://cran.r-project.org/web/packages/MethComp/MethComp.pdf

Chai, J., Herrmann, D., Stanton, M., Barbano, R., Logigian, E., 2005. Painful small-fiber neuropathy in Sjögren syndrome. Neurology 65, 925–927. https://doi.org/10.1212/01.wnl.0000176034.38198.f9

Chiang, M.-C., Lin, Y.-H., Pan, C.-L., Tseng, T.-J., Lin, W.-M., Hsieh, S.-T., 2002. Cutaneous innervation in chronic inflammatory demyelinating polyneuropathy. Neurology 59, 1094–1098.

Chien, H.-F., Tseng, T.-J., Lin, W.-M., Yang, C.-C., Chang, Y.-C., Chen, R.-C., Hsieh, S.-T., 2001. Quantitative pathology of cutaneous nerve terminal degeneration in the human skin. Acta Neuropathol. (Berl.) 102, 455–461. https://doi.org/10.1007/s004010100397

Chrisman, C.L., Platt, S.R., Chandra, A.M., deLahunta, A., Shelton, G.D., 1999. Sensory polyganglioradiculoneuritis in a dog. J. Am. Anim. Hosp. Assoc. 35, 232–235. https://doi.org/10.5326/15473317-35-3-232

Christianson, J.A., Riekhof, J.T., Wright, D.E., 2003. Restorative effects of neurotrophin treatment on diabetes-induced cutaneous axon loss in mice. Exp. Neurol. 179, 188–199. https://doi.org/10.1016/S0014-4886(02)00017-1

Collongues, N., Samama, B., Schmidt-Mutter, C., Chamard-Witkowski, L., Debouverie, M., Chanson, J.-B., Antal, M.-C., Benardais, K., de Seze, J., Velten, M., Boehm, N., 2018. Quantitative and qualitative normative dataset for intraepidermal nerve fibers using skin biopsy. PLOS ONE 13, e0191614. https://doi.org/10.1371/journal.pone.0191614

Cuddon, P.A., 2002. Acquired canine peripheral neuropathies. Vet. Clin. North Am. Small Anim. Pract. 32, 207–249. https://doi.org/10.1016/S0195-5616(03)00086-X

Cummings, J.F., de Lahunta, A., Mitchell, W.J., 1983. Ganglioradiculitis in the dog: A clinical, light- and electron-microscopic study. Acta Neuropathol. (Berl.) 60, 29–39. https://doi.org/10.1007/BF00685345

Cummings, J.F., Haas, D.C., 1966. Coonhound paralysis. An acute idiopathic polyradiculoneuritis in dogs resembling the Landry-Guillain-Barré syndrome. J. Neurol. Sci. 4, 51–81. https://doi.org/10.1016/0022-510x(67)90058-5

Datta, D., 2017. blandr: a Bland-Altman Method Comparison package for R. https://doi.org/10.5281/zenodo.824514

Davidson, E.P., Coppey, L.J., Calcutt, N.A., Oltman, C.L., Yorek, M.A., 2010. Diet-induced obesity in Sprague–Dawley rats causes microvascular and neural dysfunction. Diabetes Metab. Res. Rev. 26, 306–318. https://doi.org/10.1002/dmrr.1088

Davies, L., Spies, J.M., Pollard, J.D., McLeod, J.G., 1996. Vasculitis confined to peripheral nerves. Brain 119, 1441–1448. https://doi.org/10.1093/brain/119.5.1441

Engelstad, J.K., Taylor, S.W., Witt, L.V., Hoebing, B.J., Herrmann, D.N., Dyck, P.J.B., Klein, C.J., Johnson, D.M., Davies, J.L., Carter, R.E., Dyck, P.J., 2012. Epidermal nerve fibers: Confidence intervals and continuous measures with nerve conduction. Neurology 79, 2187–2193. https://doi.org/10.1212/WNL.0b013e3182759608

Facer, P., Mathur, R., Pandya, S.S., Ladiwala, U., Singhal, B.S., Anand, P., 1998. Correlation of quantitative tests of nerve and target organ dysfunction with skin immunohistology in leprosy. Brain 121, 2239–2247. https://doi.org/10.1093/brain/121.12.2239

Fracassi, F., 2017. Chapter 304. Canine Diabetes Mellitus, in: Ettinger, S.J., Feldman, E.C., Côté, E. (Eds.), Textbook of Veterinary Internal Medicine: Diseases of the Dog and Cat. Elsevier, St. Louis, pp. 1767–1781.

Funamoto, M., Nibe, K., Morozumi, M., Edamura, K., Uchida, K., 2007. Pathological features of ganglioradiculitis (sensory neuropathy) in two dogs. J. Vet. Med. Sci. 69, 1247–1253. https://doi.org/10.1292/jvms.69.1247

Gabriel, C.M., 2000. Prospective study of the usefulness of sural nerve biopsy. J. Neurol. Neurosurg. Psychiatry 69, 442–446. https://doi.org/10.1136/jnnp.69.4.442

Gamer, M., Lennon, J., Singh, P., 2012. Package "irr" Various coefficients of Interrater Reliability and Agreement [WWW Document]. URL https://cran.r-project.org/web/packages/irr/irr.pdf

Griffiths, I.R., Duncan, I., 1979. Distal denervating disease: a degenerative neuropathy of the distal motor axon in dogs. J. Small Anim. Pract. 20, 579–592. https://doi.org/10.1111/j.1748-5827.1979.tb06666.x

Griffiths, I.R., McCulloch, M.C., Abrahams, S., 1986. Progressive axonopathy: An inherited neuropathy of Boxer dogs. 3. The peripheral axon lesion with special reference to the nerve roots. J. Neurocytol. 15, 109–120. https://doi.org/10.1007/BF02057909

Gross, J., Ligges, U., 2015. nortest - Tests for Normality [WWW Document]. URL https://cran.r-project.org/web/packages/nortest/nortest.pdf

Hays, A.P., Harrington, W.N., Whitehouse, G., 2016. Fixation of skin biopsies for determination of epidermal nerve fiber density. Clin. Neuropathol. 35, 44–45. https://doi.org/10.5414/NP300891

Hendrix, S., Picker, B., Liezmann, C., Peters, E.M.J., 2008. Skin and hair follicle innervation in experimental models: a guide for the exact and reproducible evaluation of neuronal plasticity. Exp. Dermatol. 17, 214–227. https://doi.org/10.1111/j.1600-0625.2007.00653.x

Herrmann, D.N., Griffin, J.W., Hauer, P., Cornblath, D., McArthur, J.C., 1999. Epidermal nerve fiber density and sural nerve morphometry in peripheral neuropathies. Neurology 53, 1634–1640.

Hilton, D.A., Jacob, J., Househam, L., Tengah, C., 2007. Complications following sural and peroneal nerve biopsies. J. Neurol. Neurosurg. Psychiatry 78, 1271–1272. https://doi.org/10.1136/jnnp.2007.116368

Hilz, M.J., Axelrod, F.B., Bickel, A., Stemper, B., Brys, M., Wendelschafer-Crabb, G., Kennedy, W.R., 2004. Assessing function and pathology in familial dysautonomia: assessment of temperature perception, sweating and cutaneous innervation. Brain 127, 2090–2098. https://doi.org/10.1093/brain/awh235

Höke, A., Ho, T., Crawford, T.O., LeBel, C., Hilt, D., Griffin, J.W., 2003. Glial Cell Line-Derived Neurotrophic Factor Alters Axon Schwann Cell Units and Promotes Myelination in Unmyelinated Nerve Fibers. J. Neurosci. 23, 561–567. https://doi.org/10.1523/JNEUROSCI.23-02-00561.2003

Hopkins, W.G., 2007. New View of Statistics: Confidence Limits [WWW Document]. New View Stat. URL http://sportsci.org/resource/stats/generalize.html (accessed 4.2.20).

Hopkins, W.G., 2000. Measures of Reliability in Sports Medicine and Science. Sports Med 30, 1–15.

Hsieh, S.T., Chiang, H.Y., Lin, W.M., 2000. Pathology of nerve terminal degeneration in the skin. J. Neuropathol. Exp. Neurol. 59, 297–307. https://doi.org/10.1093/jnen/59.4.297

Hughes, R.A.C., 2014. Chapter 5: Complications from nerve biopsy., in: Vallat, J.-M., Weis, J. (Eds.), Peripheral Nerve Disorders: Pathology and Genetics. John Wiley & Sons, Oxford.

Jolivalt, C.G., Frizzi, K.E., Guernsey, L., Marquez, A., Ochoa, J., Rodriguez, M., Calcutt, N.A., 2016. Phenotyping Peripheral Neuropathy in Mouse Models of Diabetes. Curr. Protoc. Mouse Biol. 6, 223–255. https://doi.org/10.1002/cpmo.11

Kennedy, W.R., Wendelschafer-Crabb, G., Polydefkis, M., McArthur, J.C., 2005. Pathology and Quantitation of Cutaneous Innervation, in: Peripheral Neuropathy. Elsevier, pp. 869–895. https://doi.org/10.1016/B978-0-7216-9491-7.50037-5

Kiernan, J.A., 1999. Histological and histochemical methods: theory and practice.

Lakritz, J.R., Bodair, A., Shah, N., O'Donnell, R., Polydefkis, M.J., Miller, A.D., Burdo, T.H., 2015. Monocyte Traffic, Dorsal Root Ganglion Histopathology, and Loss of Intraepidermal Nerve Fiber Density in SIV Peripheral Neuropathy. Am. J. Pathol. 185, 1912–1923. https://doi.org/10.1016/j.ajpath.2015.03.007

Laprais, A., Dunston, S.M., Torres, S.M.F., Favrot, C., Olivry, T., 2017. Evaluation of intraepidermal nerve fibres in the skin of normal and atopic dogs. Vet. Dermatol. 28, 355-e80. https://doi.org/10.1111/vde.12420

Latimer, K.S., 2011. Duncan and Prasse's Veterinary Laboratory Medicine: Clinical Pathology. John Wiley & Sons, Oxford.

Lauria, G., Cornblath, D.R., Johansson, O., McArthur, J.C., Mellgren, S.I., Nolano, M., Rosenberg, N., Sommer, C., 2005a. EFNS guidelines on the use of skin biopsy in the diagnosis of peripheral neuropathy. Eur. J. Neurol. 12, 747–758.

Lauria, G., Hsieh, S.T., Johansson, O., Kennedy, W.R., Leger, J.M., Mellgren, S.I., Nolano, M., Merkies, I.S., Polydefkis, M., Smith, A.G., 2010a. European Federation of Neurological Societies/Peripheral Nerve Society Guideline on the use of skin biopsy in the diagnosis of small fiber neuropathy. Report of a joint task force of the European Fe-deration of Neurological Societies and the Peripheral Nerve Society. Eur. J. Neurol. 17, 903–912.

Lauria, G., Hsieh, S.T., Johansson, O., Kennedy, W.R., Leger, J.M., Mellgren, S.I., Nolano, M., Merkies, I.S.J., Polydefkis, M., Smith, A.G., Sommer, C., Valls-

Solé, J., 2010b. Use of Skin Biopsy in the Diagnosis of Small Fibre Neuropathy, in: European Handbook of Neurological Management. John Wiley & Sons, Ltd, Oxford, pp. 81–90. https://doi.org/10.1002/9781444328394.ch7

Lauria, G., Lombardi, R., 2012. Small Fiber Neuropathy: Is Skin Biopsy the Holy Grail? Curr. Diab. Rep. 12, 384–392. https://doi.org/10.1007/s11892-012-0280-9

Lauria, G., Lombardi, R., Borgna, M., Penza, P., Bianchi, R., Savino, C., Canta, A., Nicolini, G., Marmiroli, P., Cavaletti, G., 2005b. Intraepidermal nerve fiber density in rat foot pad: neuropathologic–neurophysiologic correlation. J. Peripher. Nerv. Syst. 10, 202–208. https://doi.org/10.1111/j.1085-9489.2005.0010210.x

Lauria, G., Morbin, M., Lombardi, R., Borgna, M., Mazzoleni, G., Sghirlanzoni, A., Pareyson, D., 2003. Axonal swellings predict the degeneration of epidermal nerve fibers in painful neuropathies. Neurology 61, 631–636.

Lauria, G., Sghirlanzoni, A., Lombardi, R., Pareyson, D., 2001. Epidermal nerve fiber density in sensory ganglionopathies: Clinical and neurophysiologic correlations. Muscle Nerve 24, 1034–1039. https://doi.org/10.1002/mus.1107

Levy, D.M., Karanth, S.S., Springall, D.R., Polak, J.M., 1989. Depletion of cutaneous nerves and neuropeptides in diabetes mellitus: an immunocytochemical study. Diabetologia 32, 427–433. https://doi.org/10.1007/BF00271262

LoMartire, R., 2020. “rel” R package [WWW Document]. URL https://cran.r-project.org/web/packages/rel/rel.pdf

Lorenz, M.D., Coates, J.R., Kent, M., 2011. Chapter 4 - Confirming a Diagnosis, in: Lorenz, M.D., Coates, J.R., Kent, M. (Eds.), Handbook of Veterinary Neurology (Fifth Edition). W.B. Saunders, Saint Louis, pp. 75–92. https://doi.org/10.1016/B978-1-4377-0651-2.10004-9

Løseth, S., Stålberg, E., Jorde, R., Mellgren, S.I., 2008. Early diabetic neuropathy: thermal thresholds and intraepidermal nerve fibre density in patients with normal nerve conduction studies. J. Neurol. 255, 1197–1202. https://doi.org/10.1007/s00415-008-0872-0

Lyubchich, V., Gastwirth, J.L., Gel, Y.R., Wallace Hui, W.L., Miao, W., Noguchi, K., 2019. lawstat Tools for Biostatistics, Public Policy and Law [WWW Document]. URL https://cran.r-project.org/web/packages/lawstat/lawstat.pdf

Mangus, L.M., Dorsey, J.L., Weinberg, R.L., Ebenezer, G.J., Hauer, P., Laast, V.A., Mankowski, J.L., 2016. Tracking Epidermal Nerve Fiber Changes in Asian Macaques: Tools and Techniques for Quantitative Assessment. Toxicol. Pathol. 44, 904–912. https://doi.org/10.1177/0192623316650286

Mangus, L.M., Rao, D.B., Ebenezer, G.J., 2019. Intraepidermal Nerve Fiber Analysis in Human Patients and Animal Models of Peripheral Neuropathy: A Comparative Review. Toxicol. Pathol. 019262331985596. https://doi.org/10.1177/0192623319855969

Mariani, C.L., 2017. Chapter 268. Peripheral Neuropathies, in: Ettinger, S.J., Feldman, E.C., Côté, E. (Eds.), Textbook of Veterinary Internal Medicine: Diseases of the Dog and Cat. Elsevier, St. Louis, pp. 1451–1456.

Maudlin, E., Peters-Kennedy, J., 2016. Chapter 6. Integumentary system, in: Maxie, M.G. (Ed.), Jubb, Kennedy & Palmer's Pathology of Domestic Animals: Volume 1 (Sixth Edition). W.B. Saunders, pp. 509–736. https://doi.org/10.1016/B978-0-7020-5317-7.00001-1

McArthur, J.C., Stocks, E.A., Hauer, P., Cornblath, D.R., Griffin, J.W., 1998. Epidermal Nerve Fiber Density: Normative Reference Range and Diagnostic Efficiency. Arch. Neurol. 55, 1513. https://doi.org/10.1001/archneur.55.12.1513

McGlone, F., Reilly, D., 2010. The cutaneous sensory system. Neurosci. Biobehav. Rev., Touch, Temperature, Pain/Itch and Pleasure 34, 148–159. https://doi.org/10.1016/j.neubiorev.2009.08.004

Mellgren, S.I., Nolano, M., Sommer, C., 2013. Chapter 10 - The cutaneous nerve biopsy: technical aspects, indications, and contribution, in: Said, G., Krarup, C. (Eds.), Handbook of Clinical Neurology, Peripheral Nerve Disorders. Elsevier, pp. 171–188. https://doi.org/10.1016/B978-0-444-52902-2.00010-2

Merkies, I.S.J., Faber, C.G., Lauria, G., 2015. Advances in diagnostics and outcome measures in peripheral neuropathies. Neurosci. Lett., Neurobiology of Peripheral Neuropathy: Current Progress 596, 3–13. https://doi.org/10.1016/j.neulet.2015.02.038

Morgan, M.J., Vite, C.H., Radhakrishnan, A., Hess, R.S., 2008. Clinical peripheral neuropathy associated with diabetes mellitus in 3 dogs. Can. Vet. J. Rev. Veterinaire Can. 49, 583–586.

Nebuchennykh, M., Løseth, S., Mellgren, S.I., 2010. Aspects of peripheral nerve involvement in patients with treated hypothyroidism. Eur. J. Neurol. 17, 67–72. https://doi.org/10.1111/j.1468-1331.2009.02743.x

Nolano, M., Biasiotta, A., Lombardi, R., Provitera, V., Stancanelli, A., Caporaso, G., Santoro, L., Merkies, I.S.J., Truini, A., Porretta-Serapiglia, C., Cazzato, D., Dacci, P., Vitale, D.F., Lauria, G., 2015. Epidermal innervation morphometry by immunofluorescence and bright-field microscopy. J. Peripher. Nerv. Syst. 20, 387–391. https://doi.org/10.1111/jns.12146

Nolano, M., Crisci, C., Santoro, L., Barbieri, F., Casale, R., Kennedy, W.R., Wendelschafer-Crabb, G., Provitera, V., Di Lorenzo, N., Caruso, G., 2000. Absent innervation of skin and sweat glands in congenital insensitivity to pain with anhidrosis. Clin. Neurophysiol. 111, 1596–1601. https://doi.org/10.1016/S1388-2457(00)00351-5

Paus, R., 1997. Neural Mechanisms of Hair Growth Control. J. Investig. Derm., Symposium Proceedings 2, 61–68.

Peters, E.M.J., Botchkarev, V.A., Botchkareva, N.V., Tobin, D.J., Paus, R., 2001. Hair-Cycle-Associated Remodeling of the Peptidergic Innervation of Murine

Skin, and Hair Growth Modulation by Neuropeptides. J. Invest. Dermatol. 116, 236–245. https://doi.org/10.1046/j.1523-1747.2001.01232.x

Peters, E.M.J., Ericson, M.E., Hosoi, J., Seiffert, K., Hordinsky, M.K., Ansel, J.C., Paus, R., Scholzen, T.E., 2006a. Neuropeptide Control Mechanisms in Cutaneous Biology: Physiological and Clinical Significance. J. Invest. Dermatol. 126, 1937–1947. https://doi.org/10.1038/sj.jid.5700429

Peters, E.M.J., Hendrix, S., Gölz, G., Klapp, B.F., Arck, P.C., Paus, R., 2006b. Nerve Growth Factor and its Precursor Differentially Regulate Hair Cycle Progression in Mice. J. Histochem. Cytochem. 54, 275–288. https://doi.org/10.1369/jhc.4A6585.2005

Popović, Z.B., Thomas, J.D., 2017. Assessing observer variability: a user's guide. Cardiovasc. Diagn. Ther. 7, 317–324. https://doi.org/10.21037/cdt.2017.03.12

Provitera, V., Gibbons, C.H., Wendelschafer-Crabb, G., Donadio, V., Vitale, D.F., Stancanelli, A., Caporaso, G., Liguori, R., Wang, N., Santoro, L., Kennedy, W.R., Nolano, M., 2016. A multi-center, multinational age- and gender-adjusted normative dataset for immunofluorescent intraepidermal nerve fiber density at the distal leg. Eur. J. Neurol. 23, 333–338. https://doi.org/10.1111/ene.12842

R Core Team, 2019. R: A Language and Environment for Statistical Computing. R Foundation for Statistical Computing, Vienna, Austria.

Ripley, B., Venables, B., 2002. MASS: Support Functions and Datasets for Venables and Ripley's MASS, 4th ed. Springer, New York.

Ross, M.H., Reith, E.J., Romrell, L.J., Kaye, G., 1995. Histology: A Text and Atlas, 3rd ed. Lippincott Williams and Wilkins, Baltimore.

Rupp, A., Galban-Horcajo, F., Bianchi, E., Dondi, M., Penderis, J., Cappell, J., Burgess, K., Matiasek, K., McGonigal, R., Willison, H.J., 2013. Anti-GM2 ganglioside antibodies are a biomarker for acute canine polyradiculoneuritis. J. Peripher. Nerv. Syst. 18, 75–88. https://doi.org/10.1111/jns5.12011

Ruts, L., van Doorn, P.A., Lombardi, R., Haasdijk, E.D., Penza, P., Tulen, J.H.M., Hempel, R.J., van den Meiracker, A.H., Lauria, G., 2012. Unmyelinated and myelinated skin nerve damage in Guillain–Barré syndrome: Correlation with pain and recovery: Pain 153, 399–409. https://doi.org/10.1016/j.pain.2011.10.037

Said, G., 2002. Indications and Usefulness of Nerve Biopsy. Arch. Neurol. 59, 1532–1535. https://doi.org/10.1001/archneur.59.10.1532

Schwarz, R., Le Roux, J.M.W., Schaller, R., Neurand, K., 1979. Micromorphology of the Skin (epidermis, dermis, subcutis) of the Dog. Onderstepoort J. Vet. Res. 46, 105–109.

Smith, A.G., Howard, J.R., Kroll, R., Ramachandran, P., Hauer, P., Singleton, J.R., McArthur, J., 2005. The reliability of skin biopsy with measurement of

intraepidermal nerve fiber density. J. Neurol. Sci. 228, 65–69. https://doi.org/10.1016/j.jns.2004.09.032

Sommer, C., 2019. Pathology of Small Fiber Neuropathy: Skin Biopsy for the Analysis of Nociceptive Nerve Fibers, in: Hsieh, S.-T., Anand, P., Gibbons, C.H., Sommer, C. (Eds.), Small Fiber Neuropathy and Related Syndromes: Pain and Neurodegeneration. Springer, Singapore, pp. 11–24. https://doi.org/10.1007/978-981-13-3546-4_2

Sommer, C., 2017. How to approach a patient with neuropathy: From diagnosis to therapy - Level 1. Nerve biopsy or skin biopsy: What to get and what to choose? Presented at the 3rd Congress of the European Academy of Neurology, European Academy of Neurology, Amsterdam.

Stefanini, M., Martino, C.D., Zamboni, L., 1967. Fixation of Ejaculated Spermatozoa for Electron Microscopy. Nature 216, 173–174. https://doi.org/10.1038/216173a0

Theerawatanasirikul, S., Suriyaphol, G., Thanawongnuwech, R., Sailasuta, A., 2012. Histologic morphology and involucrin, filaggrin, and keratin expression in normal canine skin from dogs of different breeds and coat types. J. Vet. Sci. 13, 163–170. https://doi.org/10.4142/jvs.2012.13.2.163

Torvin Møller, A., Winther Bach, F., Feldt-Rasmussen, U., Rasmussen, Å., Hasholt, L., Lan, H., Sommer, C., Kølvraa, S., Ballegaard, M., Staehelin Jensen, T., 2009. Functional and structural nerve fiber findings in heterozygote patients with Fabry disease. PAIN® 145, 237–245. https://doi.org/10.1016/j.pain.2009.06.032

Truini, A., Biasiotta, A., Onesti, E., Di Stefano, G., Ceccanti, M., La Cesa, S., Pepe, A., Giordano, C., Cruccu, G., Inghilleri, M., 2015. Small-fibre neuropathy related to bulbar and spinal-onset in patients with ALS. J. Neurol. 262, 1014–1018. https://doi.org/10.1007/s00415-015-7672-0

Tseng, M.-T., Hsieh, S.-C., Shun, C.-T., Lee, K.-L., Pan, C.-L., Lin, W.-M., Lin, Y.-H., Yu, C.-L., Hsieh, S.-T., 2006. Skin denervation and cutaneous vasculitis in systemic lupus erythematosus. Brain 129, 977–985. https://doi.org/10.1093/brain/awl010

Üçeyler, N., Kafke, W., Riediger, N., He, L., Necula, G., Toyka, K.V., Sommer, C., 2010. Elevated proinflammatory cytokine expression in affected skin in small fiber neuropathy. Neurology 74, 1806–1813.

Vlčková-Moravcová, E., Bednařík, J., Dušek, L., Toyka, K.V., Sommer, C., 2008. Diagnostic validity of epidermal nerve fiber densities in painful sensory neuropathies. Muscle Nerve 37, 50–60. https://doi.org/10.1002/mus.20889

Weir, J.P., 2005. Quantifying Test-Retest Reliability Using the Intraclass Correlation Coefficient and the SEM. J. Strength Cond. Res. 19, 231–240.

Weis, J., Katona, I., Müller-Newen, G., Sommer, C., Necula, G., Hendrich, C., Ludolph, A.C., Sperfeld, A.-D., 2011. Small-fiber neuropathy in patients with ALS. Neurology 76, 2024–2029. https://doi.org/10.1212/WNL.0b013e31821e553a

Welle, M.M., Wiener, D.J., 2016. The Hair Follicle: A Comparative Review of Canine Hair Follicle Anatomy and Physiology. Toxicol. Pathol. 44, 564–574. https://doi.org/10.1177/0192623316631843

Wöpking, S., Scherens, A., Haußleiter, I.S., Richter, H., Schüning, J., Klauenberg, S., Maier, C., 2009. Significant difference between three observers in the assessment of intraepidermal nerve fiber density in skin biopsy. BMC Neurol. 9, 13. https://doi.org/10.1186/1471-2377-9-13